Ad Hoc Networks 81 (2018) 71–85

Contents lists available at ScienceDirect

Ad Hoc Networks

journal homepage: www.elsevier.com/locate/adhoc

QoS guaranteed surveillance algorithms for directional wireless sensor networks

Chih-Yung Chang[a,*], Chih-Yao Hsiao[a], Chao-Tsun Chang[b]

[a] Department of Computer Science and Information Engineering, Tamkang University, Tamsui, New Taipei City 25137, Taiwan
[b] Department of Information Management, Hsiuping University of Science & Technology, Dali, Taichung 41280, Taiwan

ARTICLE INFO

Article history:
Received 6 April 2018
Accepted 6 June 2018
Available online 6 July 2018

Keywords:
Surveillance
QoS
***k*-Barrier coverage**
Wireless sensor networks (WSNs)

ABSTRACT

A directional wireless sensor network (DWSN) consists of a number of directional sensors. Many types of directional sensors have been widely used in constructing a wireless sensor network for IoT applications. These types of sensors include infrared sensors, microwave sensors, ultrasonic sensors, cameras, and radar. Compared with an omni-directional sensor, a directional sensor can achieve better performance because it can additionally report the direction of an intruder. Unfortunately, most existing barrier-coverage mechanisms adopt omni-directional sensor networks. They cannot be efficiently applied to DWSNs because the sensing area of each directional sensor is fan-shaped. This paper investigates the surveillance service problem which supports the surveillance quality of k-barrier coverage in DWSNs. Three algorithms, called BA, BTA and BRA, are proposed which aim at finding a maximal number of different defense barriers, each of which supports k-coverage. Using these algorithms, at least k directional sensors can detect intruders intending to cross the monitoring area. Performance analyses of the proposed algorithms are conducted in Section 5 to verify the performance improvement from a theoretical point of view. In the performance study, the proposed algorithms are compared with other existing algorithms. The experimental study shows that the proposed k-barrier coverage algorithm achieves similar performance with the optimal solution but has fewer control packets. Furthermore, the proposed BRA achieves better performance in terms of the numbers of control packets and constructed defense barriers, as compared with existing algorithms.

1. Introduction

Directional wireless sensor networks (DWSNs) consist of a number of directional sensors. The directional sensors have been widely used for IoT applications [1–5]. These applications include supporting visual monitoring services [1,2], identifying the positions of objects [3], and constructing a virtual fence [4,5] on the border between Mexico and the United States. The k-barrier coverage problem [6–13] has been widely discussed for wireless sensor networks (WSNs) in the past few years. A defense barrier constructed by a set of sensors in a given monitored region R is said to satisfy k-barrier coverage if any crossing path is covered by at least k distinct sensors [6], where a path is said to be a crossing path if the path crosses through the complete width of R. Compared with a traditional sensor in WSNs, each directional sensor in DWSNs is equipped with an infrared sensor, a microwave sensor, an ultrasonic sensor, a camera, radar, and so on, which provides rich information for better understanding the behavior of targets in target tracking applications. Being different from traditional sensor, the sensing range of a directional sensor is a Field of View (FoV), which can be viewed as fan-shaped. Hence the existing barrier-coverage algorithms [6–14] developed for WSNs cannot be applied to DWSNs.

In the past few years, barrier coverage problem in DWSNs has attracted much attention [15–22]. Since considerable intrusive information captured by directional sensors will be further processed by the sink node, most of the existing approaches [15–21] aim to reduce the number of active directional sensors for reducing the computing loads at the sink and energy consumptions at sensor nodes. Ma et al. [15] analyzed the FoV sensing model of directional sensors and then proposed a connectivity checking and repairing method, aiming to maintain the connectivity between directional sensors. However, the authors did not take into consideration the construction of defense barrier. Several studies [16–19] have proposed barrier construction algorithms. The main concept is that the contribution of each directional sensor is transformed into a

* Corresponding author.
E-mail addresses: cychang@mail.tku.edu.tw (C.-Y. Chang), cyhsiao@gms.tku.edu.tw (C.-Y. Hsiao), cctas@mail.hust.edu.tw (C.-T. Chang).

https://doi.org/10.1016/j.adhoc.2018.06.007
1570-8705/

partial barrier line. The set of directional sensors that contribute to the largest partial barrier line will be selected. The length of the partial barrier line can be enlarged if two partial barrier lines overlap. As a result, the barrier can be constructed from the leftmost to the rightmost boundaries. However, these studies did not consider the k-barrier coverage problem, for $k \geq 2$. Also, the maximal number of constructed defense barriers was not achieved.

Moreover, studies [20,21] proposed centralized barrier-coverage algorithms aiming to minimize the number of directional sensors. Wang et al. [20] transformed the given monitored region into a weighted graph. An approach based on the Hungarian Algorithm is applied to find the barrier lines on the weighted graph. As an extension of study [20], Wang et al. [21] further demonstrated that constructing a defense barrier with k-barrier coverage is related to finding k vertex-disjoint paths on a weighted graph. An algorithm based on Menger's Theorem was proposed for finding the k vertex-disjoint paths. However, the efficiencies of these centralized algorithms [15,16,18,20,21] could be further improved since they raise considerable communication overhead for collecting the locations and FoV information from all directional sensors.

This paper addresses the k-barrier coverage problem and develops a decentralized k-Barrier Coverage Construction (k-BCC) mechanism for DWSNs. The developed k-BCC mechanism aims to construct the maximal number of distinct defense barriers. Each constructed defense barrier is composed of as few directional sensors as possible while satisfying the cover requirement of k-barrier coverage. In the proposed k-BCC mechanism, the given monitored region will be initially partitioned into several equal-sized grids for simplifying the k-barrier coverage problem. Then a Basic Approach (BA) is proposed aiming at constructing a number of defense barriers. Each of the constructed defense barriers consists of a minimum number of directional sensors but satisfies the k-barrier coverage. Based on the proposed BA, the Backtracking Approach (BTA) and Branch Approach (BRA) are further proposed to construct more defense barriers with the capability of k-barrier coverage. Consequently, those directional sensors that participate in the constructed defense barriers can work in turn and the load balance purpose can be achieved.

The following presents the main contributions of this paper.

1) **Proposing a decentralized solution which achieves similar performance to the centralized optimal solution.** By locally considering the contribution of each directional sensor, the proposed decentralized k-BCC mechanism can construct a satisfactory number of distinct defense barriers. Each constructed barrier consists of as few directional sensors as possible but still guarantees k-barrier coverage. In comparison, we treat MDP [23] as the optimal solution since it is centralized and uses exhausted search for all possible solutions. The proposed BRA mechanism achieves similar performance as the optimal solution while the number of control packets of BRA is significantly reduced.
2) **Achieving better performance than existing works.** The proposed BRA mechanism outperforms existing distributed algorithms CoBRA [17] and D-TriB [19], and centralized algorithms MNBG [21] and MDP [23] in terms of the number of control packets.
3) **Overcoming the obstacle problem.** The dead-end problem might occur when constructing a barrier. The proposed BTA and BRA adopt the backtracking and branch approaches to overcome the dead-end problem and further find more feasible solutions for constructing the defense barriers. Hence both of BTA and BRA can be applied to the obstacle environment. To our knowledge, this is the first decentralized algorithm that handles the dead-end problem when constructing a barrier.
4) **Handling the heterogeneous problem.** The proposed k-BCC mechanism can be also applied in heterogeneous directional sensor networks because each directional sensor just needs to calculate its contribution for constructing the defense barrier based on parameters including its sensing radius, field of view, view angle, and coordinates.
5) **Flexibility**. The proposed BA, BTA, and BRA approaches can work independently or can be integrated, according to the situations of a given monitored region. Compared with related works [15,16,18,20,21], the proposed approaches have more flexibility.
6) **Problem simplification and performance analysis.** The proposed k-BCC mechanism which partitions the monitoring region into a number of grids can further simplify the barrier construction problem and reduce the computational complexity. Theoretical analyses of performance drop caused by *grid partition* and message complexity are also made in Section 5.

The remainder of this paper is organized as follows. Section 2 discusses related works. Section 3 introduces the network environment and problem statement. Section 4 gives the detailed description of the proposed mechanisms. Section 5 gives a theoretical analysis for verifying the performance of the proposed barrier-coverage approaches. Section 6 presents the simulation results while Section 7 concludes this paper.

2. Related work

Barrier coverage is one of the most important topics in wireless sensor networks, which can be implemented in several applications including national border control, critical resource protection as well as intruder detection. In a WSN, a defense barrier is formed by selecting a set of sensors whose sensing ranges are contiguous and span across the monitored field. Every object crossing the field from one side to another will be detected by at least one sensor on the defense barrier. The following subsection presents related literature on barrier coverage developed for WSNs and directional WSNs.

2.1. Barrier coverage in WSNs

The barrier coverage problem for traditional WSNs has been studied extensively in the past few years. Kumar et al. [6] firstly defined the notion of k-barrier coverage of a belt region for wireless sensors. They proposed an algorithm to determine whether a belt region supports the k-barrier coverage. Kumar et al. [7] further proposed a centralized sleep-wake-up schedule, aiming to prolong the lifetime of the performing barrier for wireless sensors. Chen et al. [8] introduced the concept of local barrier coverage for WSNs. They proposed a sleep-wakeup algorithm, aimed at maximizing the network lifetime. Huang et al. [9] proposed a centralized algorithm for constructing the barrier for WSNs. In the proposed algorithm, the boundary arcs of the sensing intersection area among sensors were calculated. A set of sensors with large projection lengths were selected to form the barrier. Yang et al. [10] investigated the effectiveness of sensing range of each sensor on barrier and derived the projection length of each sensor. A centralized scheme which combines all the projection lengths was developed for constructing the barrier.

Liu et al. [11] divided the monitoring region into several horizontal rectangular segments interleaved by vertical thin strips. Each segment and vertical strip independently forms the local horizontal and vertical barriers, respectively. The barrier for the whole region is constructed if neighboring local horizontal and vertical barriers were connected with each other. Chen et al. [12] proposed a mechanism that measures the quality of the barrier. If the quality of the barrier falls below a desired level, they further proposed a method to identify all the weak zones. Then a repair algorithm is obtained to repair the weak zones until the barrier achieves a desired level. He et al. [13,14] introduced a notion of distance-continuous and then designed sensor deployment algorithms for barrier coverage in WSNs. However, the abovementioned studies were developed for omni-directional sensors only. They cannot be efficiently applied to DWSNs because the sensing area of each directional sensor is fan-shaped. Furthermore, most of the abovementioned mechanisms were centralized, which require collecting the locations of the sensors and then making a decision. The proposed algorithms here are decentralized, where each sensor only needs to collect information from the neighboring sensor. Compared with the abovementioned existing studies, the proposed decentralized algorithms further support scalability and flexibility.

2.2. Barrier coverage in directional WSNs

Recently, the barrier coverage problem for directional WSNs has gradually received much attention. Ma et al. [15] analyzed deployment strategies with a FoV sensing model for directional sensors. They proposed connectivity checking and repairing methods, aiming to maintain the connectivity between directional sensors. However, the authors did not take into consideration the construction of a defense barrier. Zhang et al. [16] firstly transformed the given monitored region into a coverage graph. Based on the coverage graph, the authors presented an integer linear programming formula for modeling the barrier coverage problem and then proposed a centralized algorithm to find the defense barriers. The authors also came up with a decentralized defense barrier construction algorithm where a defense barrier is constructed by combining barrier fragments. Shih et al. [17] proposed a distributed algorithm, aiming to construct the barrier in wireless camera sensor networks. In the proposed algorithm, the contribution of each camera sensor on the barrier is transformed into a partial barrier line. The set of camera sensors that contributes the largest partial barrier line will be selected. The length of the partial barrier line can be enlarged if two partial barrier lines overlap. As a result, the barrier can be constructed from the leftmost to the rightmost boundaries. Cheng and Tsai [19] initially converted the FoV of each directional sensor into a horizontal line. Later on, a directional sensor located at the leftmost boundary is selected to be the initiator. Based on the length of the horizontal line, the initiator selects suitable relay directional sensors from left to right until the rightmost boundary is reached. However, previous works [16–19] did not consider the k-barrier coverage problem for $k \geq 2$. To our knowledge, the maximal number of constructed defense barriers is never achieved.

Wang et al. [20] introduced the notion of a weighted barrier graph (WBG) to model the barrier coverage problem. They demonstrated the concept that the minimum number of directional sensors required to form a defense barrier with 1-barrier coverage is the length of the shortest path from the source node to the destination node on the WBG. An approach based on the Hungarian algorithm is proposed to solve the problem of 1-barrier coverage. As an extension of study [20], Wang et al. [21] further proved the fact that the minimum number of directional sensors required to form a defense barrier with k-barrier coverage is related with finding k vertex-disjoint paths with the minimum total length on the WBG. Afterwards, an algorithm based on a previous work, called Vertex-Disjoint Path Approach, is proposed for solving the problem of k-barrier coverage. However, the efficiency of these centralized algorithms [15,16,18,20,21] could be further improved since they raise considerable communication overhead for collecting the locations and FoV information from all directional sensors. Table 1 summarizes the characteristics of the existing algorithms and the proposed k-BCC.

3. Network environment and problem statement

This section initially introduces the network environment and assumptions of the considered DWSNs. Later, the problem formulations of this work are proposed.

3.1. Network environment

The considered monitoring area is a rectangle region R with size $L \times W$, where L and W are the length and width of R, respectively. Let notations L_{top}, L_{bottom}, W_{left}, and W_{right} denote the top, bottom, left, and right boundaries of R, respectively. A path is said to be a *crossing path* if it completely crosses from L_{bottom} to L_{top}. A set of n directional sensors $V=\{v_1,v_2,\ldots, v_n\}$ are randomly deployed in R. Each directional sensor v_i has a unique ID and is aware of its own location and the boundaries of R. Each v_i has a non-rotatable *sensing range* with sensing radius r, communication radius $2r$, field-of-view (FoV) angle θ, and orientation vector ϕ_i. The energy required for each v_i is sufficiently supported. This can be achieved by many existing Energy Harvesting technologies [24]. Through exchange of beacon messages with one-hop neighbors, each v_i can collect IDs, locations, and information of sensing range of its neighboring directional sensors. A notation table is given below to summarize notations used in the proposed k-BCC mechanism (Table 2).

3.2. Problem formulation

Let $DB_h^1 = (v_{\hat{1}}, v_{\hat{2}}, \ldots, v_{\hat{f}_h})$ denote the hth constructed *defense* 1-*coverage barrier* which is composed of $\hat{f}_h$ ordered directional sensors, where $v_{\hat{i}}$ denotes the ith directional sensor participating in DB_h^1, when applying a certain algorithm. The definitions of Initiator and Terminator, and *disjoint k-coverage barrier* are given below.

Definition 1. Initiator and Terminator; $v_{\hat{1}}$ and $v_{\hat{f}_h}$

The Initiator, denoted by $v_{\hat{1}}$, is the first sensor participating in the construction of DB_h^1 and its sensing range intersects with W_{left}. The Terminator, denoted by $v_{\hat{f}_h}$, is the last sensor participating in the constructing of DB_h^1 and its sensing range intersects with W_{right}.□

Definition 2. Disjoint k-Coverage Barrier; DB^k

A disjoint k-coverage barrier, denoted by DB^k, is a collection of k disjoint DB^1s. That is,

$$DB^k = \bigcup_{h=1}^{k} DB_h^1 \tag{1}$$

□

The construction of a DB^k can be achieved by finding k *disjoi* DB^1s. The following presents several constraints that should be satisfied during the construction of a DB^k.

In the k-barrier coverage problem, any crossing path should be detected by at least k directional sensors in the given monitoring region R. The proposed k-BCC mechanism aims to solve the problem of k- barrier coverage. The following presents the objective function and the constraints of the k-barrier coverage problem.

Let N denote the number of disjoint k-coverage barriers that can be constructed in R by applying a certain algorithm. As shown in (2), the objective function of this paper is constructing the maximum number of disjoint defense barriers each of which supports k-barrier coverage.

$$\textbf{maximize} \ (N) \tag{2}$$

Expression (2) also indicates that the number of directional sensors that compose each DB^k should be minimized in order to maximize the number of constructed disjoint k-coverage barriers. This

Table 1
Main characteristics of the k-BCC and related algorithms.

Studies	Directional WSNs	Barrier Construction	Decentralized Algorithm	k-Barrier Coverage	Flexibility
[6,11]	X	X	X	V	X
[7–10,12–14]	X	X	X	V (1-Cover)	X
[15,18,20]	V	X	X	V (1-Cover)	X
[16,17,19]	V	V	V	V (1-Cover)	X
[21]	V	X	X	V	X
k-BCC	V	V	V	V	V

Table 2
Notation table.

Notations	Descriptions
DB^k	The Disjoint k-Coverage Barrier
$g_{x,y}$	A grid with coordinates (x, y).
$g^{curr}_{x,y}$	The $g_{x,y}$ that is currently considered by the proposed algorithms.
$DM^{curr}_{x,y}$	The sensor that plays the role of Decision Maker of $g^{curr}_{x,y}$.
$q^{k,j}_{x,y}$	The jth candidate working set of $g_{x,y}$, which is composed of k directional sensors.
$Q^{k,m}_{x,y}$	The m possible candidate working sets of $g_{x,y}$, each of which is composed of k directional sensors.
$\hat{q}^{k}_{x,y}$	The best working set in $Q^{k,m}_{x,y}$.
$g^{k,j,x,y}_{\rho,\sigma}$	The *extended grid* of $q^{k,j}_{x,y}$ if both $g^{curr}_{x,y}$ and $g^{k,j,x,y}_{\rho,\sigma}$ are fully covered by all of the directional sensors in $q^{k,j}_{x,y}$.
$g^{BestEnding}_{\alpha,\beta}$	The grid $g^{k,j,x,y}_{\rho,\sigma}$ that has maximal weighted distance d to $g^{curr}_{x,y}$.
S_n, S_{n+1}	The *current constructed segment* and the *next constructed segment*.
$g^{next}_{x',y'}$	The *starting grid* of S_{n+1}.
$g^{k,j,x,y}_{\alpha+\zeta,\beta+\xi}$	The *candidate starting grids* of S_{n+1}, where $-1 \le \zeta \le 1$ and $-1 \le \xi \le 1$.
$DM^{next}_{x',y'}$	The DM of $g^{next}_{x',y'}$.
$DM^{prev}_{x,y}$	The previous DM of $g^{curr}_{x,y}$.
G	$G=\{g_1, g_2, \ldots, g_\eta\}$ has η weak grids selected by $DM^{curr}_{x,y}$.
c_ω	The coverage degree of grid g_ω, where $g_\omega \in G$.

goal can reduce the complexities of intrusive information computing and communication. Since the constructed k-coverage barriers can work in turn, the reliability of intruder detection task can also be significantly improved when the number of constructed k-coverage barriers is increased.

Let $v^{sen}_{\hat{i}}$ denote the sensing range of the ith directional sensor in DB^1_h. Constraint (3) shows that the sensing ranges of two neighboring directional sensors in DB^1_h should be overlapped.

Continuous constraint:

$$v^{sen}_{\hat{i}} \cap v^{sen}_{\hat{i}+1} \neq \varnothing,\ \ 1 \le \hat{i} \le \hat{f}_h - 1,\ \ \forall v_{\hat{i}}, v_{\hat{f}_h} \in DB^1_h \tag{3}$$

Another constraint, called *boundary constraint*, should be satisfied for the first directional sensor $v_{\hat{1}}$ and last directional sensor $v_{\hat{f}_h}$ in DB^1_h. As expressed in (4), the sensing range of the first sensor $v^{sen}_{\hat{1}}$ should overlap with the left boundary of R (i.e., W_{left}) and the sensing range of the last sensor, denoted by $v^{sen}_{\hat{f}_h}$, should overlap with W_{right}.

Boundary constraint:

$$v^{sen}_{\hat{1}} \cap W_{left} \neq \emptyset \ \wedge\ v^{sen}_{\hat{f}_h} \cap W_{right} \neq \emptyset, \forall v_{\hat{1}}, v_{\hat{f}_h} \in DB^1_h \tag{4}$$

Let $x_{i,h}$ denote the *Boolean* value indicating whether or not the v_i participates in DB^1_h. That is,

$$x_{i,h} = \begin{cases} 1, & \text{if } v_i \in DB^1_h \\ 0, & \text{otherwise} \end{cases}. \tag{5}$$

Recall that the *notations* L and V denote the length of R and the set of directional sensors deployed in R, respectively. Constraint (6) states that each v_i participates in at most one defense 1-coverage barrier. In other words, any two defense 1-coverage barriers, says DB^1_α and DB^1_β, should be sensor-disjoint.

Sensor-disjoint constraint:

$$\sum_{\forall DB^1_h} x_{i,h} \le 1,\ \ \forall i \in V \tag{6}$$

The following explains the reason why the k DB^1s that construct a DB^k should be sensor-disjoint. Consider a DB^2, which consists of two DB^1s, say DB^1_α and DB^1_β. If DB^1_α and DB^1_β. share a common sensor, the crossing path might pass through this sensor and hence only one sensor can detect the intruder. As a result, DB^2 can only contribute 1-coverage.

The next section presents the proposed k-BCC which aims to achieve the goal given in (2) while satisfying (3), (4), and (6).

4. The proposed *k*-Barrier Coverage Construction mechanism (*k*-BCC)

The proposed k-BCC mechanism consists of two phases. In the *initialization phase*, the given region R is partitioned into a number of equal-sized grids for simplifying the k-barrier coverage problem. Then the second phase, called *barrier construction phase*, aims to construct a DB^k grid by grid from W_{left} to $W_{right.}$

4.1. Initialization phase

Each directional sensor v_i has two major tasks to be accomplished. The first task is *region partitioning* which aims to partition the given region R into a set of equal-sized grids as shown in Fig. 1. Let the size of grid be $l \times l$. Each grid is assigned with coordinates (x, y). As shown in Fig. 1, the topmost left grid is assigned with coordinates (1, 1) and the x-coordinate and y-coordinate are increased by one if the location of a grid shifts one position towards the right and the down direction, respectively. Let notation $g_{x,y}$ represent a grid with coordinates (x, y). Each v_i in this phase will firstly identify the coordinates of its own located grid.

Let notation $\hbar$ denote the maximum size of the square that can be contained in the sensing range of a directional sensor. The size of grid ℓ is bounded by $0 < \ell \le \hbar$. This makes it possible that the grid can be fully covered by the directional sensor. The size of the grid is a tradeoff between computational complexity and construction preciseness. A larger grid size can reduce the computational

	1	2	3			l
1	(1,1)	(2,1)	(3,1)	…	…	(l,1)
2	(1,2)					
⋮	⋮					
w	(1,w)					

Fig. 1. Grid-based partition.

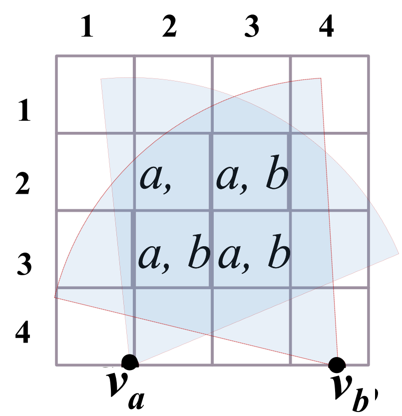

Fig. 2. The fully covered grids of v_a and v_b.

complexity of each directional sensor but will lead to a drop in the performance. This occurs because a large-sized grid can reduce the number of sensors that fully cover one grid, which reduces the number of sensors that can participate in the barrier-construction task. It is obvious that when the grid size is degraded to a certain point, it is equivalent to removing the grid. Here, we assume that the size of the grid is small enough such that the sensing range of each directional sensor can fully cover at least one grid. Section 5 presents the analysis of the performance drop caused by *grid partition*. Section 6 further offers several simulations to investigate the impact of grid size on performance in terms of the degree of performance drop and the success ratio of defense 3-coverage barrier construction.

The second task of each v_i is *coverage identification*. Here, we notice that a grid might be commonly and fully covered by the sensing ranges of several directional sensors. Therefore, in the initialization phase, each v_i should evaluate the *coverage degrees* of those grids covered by itself. The following defines *Fully Covered Set of* v_i.

Definition 3. Fully Covered Set of v_i; G_i

A grid $g_{x,y}$ is said to be a fully covered grid of v_i if the grid $g_{x,y}$ is fully covered by v_i. The fully covered set of v_i, denoted by G_i, consists of all fully covered grids of v_i. □

Fig. 2 gives an example of G_i. In Fig. 2, the grids that are fully covered by v_a and v_b are marked with notations a and b, respectively. Therefore, we have $G_a = \{g_{2,2}, g_{2,3}, g_{3,2}, g_{3,3}\}$ and $G_b = \{g_{2,3}, g_{3,2}, g_{3,3}\}$.

By exchanging the fully covered set with neighbors, each v_i can derive the coverage degree of grids that belong to G_i. More specially, a grid $g_{x,y}$ is said to be p-covered if the grid $g_{x,y}$ is fully covered by p different directional sensors. In other words, a $g_{x,y}$ is p-covered if and only if the coverage degree of $g_{x,y}$ is p.

4.2. Barrier construction (BC) phase

This section presents the construction of DB^k. In a conceptual level, a DB^k is composed of a series of interconnected *segments*. Each segment consists of several k-covered grids contributed by k directional sensors. Let *starting grid* and *ending grid* be the leftmost and rightmost grids of a segment, respectively. Two segments are said to be *interconnected* if the starting grid of the successive segment neighbors is connected to the ending grid of the previous segment. As a result, a DB^k can be constructed by connecting a series of interconnected segments. The BC phase will construct a DB^k segment by segment from boundaries W_{left} to W_{right}.

To accomplish a DB^k in each segment, a directional sensor is selected to be the *Decision Maker* (DM) for executing the operations proposed in the BC phase. Consider a grid $g_{x,y}$. All of the directional sensors that can fully cover $g_{x,y}$ are called DM candidates of $g_{x,y}$. One of them will play the role of DM of grid $g_{x,y}$ if it has the largest number of neighbors in DM candidates of $g_{x,y}$. In case that there is more than one directional sensor having the same number of neighbors, the one with the largest ID will play the role of DM. In the BC phase, three approaches, the *Basic Approach* (BA), *Backtracking Approach* (BTA), and *Branch Approach* (BRA), are developed to implement the BC phase. Each DM applies the proposed approaches aiming to construct DB^k.

The defense barrier can be constructed by locally exchanging construction message among DMs from W_{left} to W_{right}. The *first DM*, which is treated as an Initiator $v_{\hat{1}}$, is the DM that initializes the construction of each defense barrier based on the proposed BA, BTA, and BRA. The DM is said to be the *Initiator candidate* if there exists a grid $g_{1,y}$, $1 \le y \le$ w, belonging to its fully covered set, and have not yet participated in the construction of any defense barrier. Each Initiator candidate should determine a particular time period, called *delay time*. The delay time t_i of an initiator candidate DM_i is set by $t_i = (y-1) \times \lambda$, where λ is a predefined time slot and y is the y-axis coordinates of the grid $g_{x,y}$ that satisfies $g_{x,y}$ is the closest grid in G_i to the upper-left grid $g_{1,1}$. Herein, we guarantee that all Initiator candidates should have different delay times, since each Initiator candidate should cover grid $g_{1,y}$, and each $g_{1,y}$ is in charge of at most one DM.

After calculating the delay time, each Initiator candidate should execute an *Initiator competition process*, where each initiator candidate waits for its own delay time before accessing the medium. When the delay time has expired, the Initiator candidate can broadcast an *Initiator message*, aiming to notify all the initiator candidates that it is an Initiator. The Initiator candidates that receive the Initiator message should abandon the Initiator competition process. The Initiator then starts to construct the defense barrier according to the proposed BA, BTA, and BRA. The defense barrier can be constructed segment by segment until the DM, say DM_j, that plays the role of Terminator $v_{\hat{f}_h}$. The DM_j which satisfies the following two criteria can play the Terminator role: (1) DM_j has not yet participated in any construction of a defense barrier; (2) DM_j has at least a fully covered grid $g_{l,y}$, $1 \le y \le$ w, which belongs to its fully covered set. Once the defense barrier is constructed, the Terminator will notify the Initiator about the success of constructing the defense barrier. All the Initiator candidates will again execute the Initiator competition process, aiming to play the Initiator role for constructing the next defense barrier until there does not exist any Initiator candidate.

In the developed k-BCC mechanism, three barrier-construction policies, called BA, BTA, and BRA are proposed. Firstly, a decentralized BA mechanism is proposed to deal with the k-barrier coverage problem, which is simple and easy to be implemented. In addition to BA, the BTA and BRA algorithms that adopt backtracking and branch policies are proposed to further construct more disjoint

k-coverage barrier (DB^k) than BA. Compared with BA, the BTA provides more opportunities for successfully constructing the DB^k. The BRA can use up many directional sensors as possible for constructing the maximum number of DB^k.

1) Basic Approach (BA)

This section describes the proposed BA for constructing a DB^k. Recall that a DB^k is constructed in a segment by segment manner from W_{left} to W_{right}. Let $g_{x,y}^{curr}$. denote the $g_{x,y}$ which is currently considered by algorithm BA. Let $DM_{x,y}^{curr}$ denote the DM of $g_{x,y}^{curr}$. The $DM_{x,y}^{curr}$ only considers a $g_{x,y}^{curr}$ at a time and tries to find the best set of k directional sensors, which is referred to the *best working set* $\hat{q}_{x,y}^{k}$ of $g_{x,y}^{curr}$. Initially, the $DM_{x,y}^{curr}$ will find each candidate working set which consists of k directional sensors and each of them can fully cover grid $g_{x,y}^{curr}$. Let $q_{x,y}^{k,j}$ denote the jth candidate working set found by $DM_{x,y}^{curr}$. Let $Q_{x,y}^{k,m}$ denote the set of m possible *candidate working sets* $q_{x,y}^{k,j}$. That is,

$$Q_{x,y}^{k,m} = \left\{ q_{x,y}^{k,j} | 1 \le j \le m \right\} \tag{7}$$

Then the $DM_{x,y}^{curr}$ will select one best working set $\hat{q}_{x,y}^{k}$ from set $Q_{x,y}^{k,m}$. The selection policy for finding $\hat{q}_{x,y}^{k}$ is called *Best Working Set Construction Process* which is presented below.

a) Best Working Set Construction Process

The following explains how $DM_{x,y}^{curr}$ selects the best working set $\hat{q}_{x,y}^{k}$ from $Q_{x,y}^{k,m}$. The policy for determining the $\hat{q}_{x,y}^{k}$ is based on the contribution of each candidate working set $q_{x,y}^{k,j}$ in $Q_{x,y}^{k,m}$. Let $g_{\rho,\sigma}^{k,j,x,y}$ denote an *extended grid* of $q_{x,y}^{k,j}$ if both $g_{x,y}^{curr}$ and $g_{\rho,\sigma}^{k,j,x,y}$ are fully covered by all of the directional sensors in $q_{x,y}^{k,j}$. Let $Max(W, L)$ denote the maximum value between W and L, where W and L are the width and length of the given monitored region R, respectively. Let *weighted distance* d between the extended grids $g_{\rho,\sigma}^{k,j,x,y}$ and $g_{x,y}^{curr}$ be evaluated by applying (8).

$$d\left(g_{x,y}^{curr}, g_{\rho,\sigma}^{k,j,x,y}\right) = (y - \sigma) + (\rho - x) \cdot Max(W, L) \tag{8}$$

The grid $g_{\rho,\sigma}^{k,j,x,y}$ closer to boundary W_{right} has a larger weighted distance d and thus is considered having a larger contribution. This occurs because the weighted distance d is the length of the defense barrier contributed by the working set $q_{x,y}^{k,j}$. A larger d means that the defense barrier requires fewer directional sensors to be accomplished. In (8), the multiplication of $Max(W, L)$ and $(\rho - x)$ is to emphasize the weighted distance increasing in the x-axis direction since a straight defense barrier is the most appropriate in constructing the defense barrier.

As shown in (9), the $g_{\rho,\sigma}^{k,j,x,y}$ that has maximal weighted distance to grid $g_{x,y}^{curr}$, denoted by $g_{\alpha,\beta}^{BestEnding}$, will be the best ending grid of the current segment.

$$g_{\alpha,\beta}^{BestEnding} = \arg\ max\ d\left(g_{x,y}^{curr}, g_{\rho,\sigma}^{k,j,x,y}\right) \tag{9}$$

Therefore, the candidate working set $q_{x,y}^{k,j}$ that can fully cover the grid $g_{\alpha,\beta}^{BestEnding}$ has the largest contribution and will be selected as the best working set $\hat{q}_{x,y}^{k}$ by $DM_{x,y}^{curr}$. The grids covered by all directional sensors in $\hat{q}_{x,y}^{k}$ will become defense grids. These defense grids are regarded as a constructed segment of DB^k and any directional sensor in the best working set $\hat{q}_{x,y}^{k}$ will not be considered again in the following segment construction.

Recall that a DB^k is constructed segment by segment. The current grid $g_{x,y}^{curr}$. and the best ending grid $g_{\alpha,\beta}^{BestEnding}$ will be the starting grid and ending grid of the constructed segment, respectively. The next step of BA is to construct the next segment which connects to the previous one. Let $g_{x',y'}^{next}$ denote the *starting grid of the next segment*. To accomplish this, the $DM_{x,y}^{curr}$ will select a proper $g_{x',y'}^{next}$. Then the *best working set construction process* and the $g_{x',y'}^{next}$ selection process (discussed later), will be repeatedly performed to construct the defense barrier segment by segment. As a result, the DB^k can be constructed by repeatedly executing the above-mentioned procedure until a constructed segment reaches the boundary W_{right}.

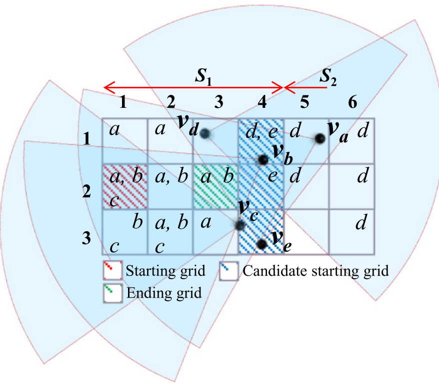

Fig. 3. An example for illustrating the construction of a DB^2 by applying BA.

Fig. 3 is an example of selecting the best working set. As shown in Fig. 3, the fully covered sets of v_a, v_b, v_c, v_d and v_e are $G_a = \{g_{1,1}, g_{1,2}, g_{2,1}, g_{2,2}, g_{2,3}, g_{3,2}, g_{3,3}\}$, $G_b = \{g_{1,2}, g_{1,3}, g_{2,2}, g_{2,3}, g_{3,2}\}$, $G_c = \{g_{1,2}, g_{1,3}, g_{2,3}\}$, $G_d = \{g_{4,1}, g_{5,1}, g_{5,2}, g_{6,1}, g_{6,2}, g_{6,3}\}$ and $G_e = \{g_{4,1}, g_{4,2}\}$, respectively. The grid $g_{1,2}$ is the starting grid which has $w = 3$ candidate working sets: $q_{1,2}^{2,1} = \{v_a, v_b\}$, $q_{1,2}^{2,2} = \{v_a, v_c\}$ and $q_{1,2}^{2,3} = \{v_b, v_c\}$. The extended grids of $q_{1,2}^{2,1}$, $q_{1,2}^{2,2}$ and $q_{1,2}^{2,3}$ are $\{g_{1,2}^{2,1,1,2}, g_{2,2}^{2,1,1,2}, g_{2,3}^{2,1,1,2}, g_{3,2}^{2,1,1,2}\}$, $\{g_{1,2}^{2,2,1,2}, g_{2,3}^{2,2,1,2}\}$ and $\{g_{1,2}^{2,3,1,2}, g_{1,3}^{2,3,1,2}, g_{2,3}^{2,3,1,2}\}$, respectively. The farthest extended grid of $q_{1,2}^{2,1}$. , $q_{1,2}^{2,2}$ and $q_{1,2}^{2,3}$ are $g_{3,2}^{2,1,1,2}$, $g_{1,2}^{2,2,1,2}$ and $g_{2,3}^{2,3,1,2}$, respectively. By applying (8) and (9), the contributions of $q_{1,2}^{2,1}$, $q_{1,2}^{2,2}$ and $q_{1,2}^{2,3}$ are evaluated below.

$$q_{1,2}^{2,1} : d\left(g_{1,2}^{curr}, g_{3,2}^{2,1,1,2}\right) = (2-2) + (3-1) \cdot Max(3, 6) = 12$$

$$q_{1,2}^{2,2} : d\left(g_{1,2}^{curr}, g_{2,3}^{2,2,1,2}\right) = (2-3) + (2-1) \cdot Max(3, 6) = 5$$

$$q_{1,2}^{2,3} : d\left(g_{1,2}^{curr}, g_{2,3}^{2,3,1,2}\right) = (2-3) + (2-1) \cdot Max(3, 6) = 5$$

As a result, the $g_{\alpha,\beta}^{BestEnding}$ will be the $g_{3,2}$ and the $q_{1,2}^{2,1} = \{v_a, v_b\}$ be selected as the best working set, say $\hat{q}_{1,2}^{2} = \{v_a, v_b\}$, in charge of monitoring the $Segment_1$ between $g_{1,2}$ and $g_{3,2}$.

The following presents how $DM_{x,y}^{curr}$ selects the next starting grid for initiating the construction of the next segment.

b) Next Starting Grid Selection Process

This paragraph describes how $DM_{x,y}^{curr}$ selects the starting grid of the next segment $g_{x',y'}^{next}$. Let S_n and S_{n+1} denote the current constructed segment and the next segment, respectively. Recall (9) that $g_{\alpha,\beta}^{BestEnding}$ denotes the best ending grid of S_n. The $g_{x',y'}^{next}$ should be able to connect to the best ending grid $g_{\alpha,\beta}^{BestEnding}$ of S_n. Let $g_{\alpha+\zeta,\beta+\xi}^{k,j,x,y}$, where $-1 \le \zeta \le 1$ and $-1 \le \xi \le 1$ denote the *candidate starting grids* of S_{n+1}. Obviously, each candidate starting grid $g_{\alpha+\zeta,\beta+\xi}^{k,j,x,y}$ of S_{n+1} should be k-covered and will be connected to the best ending grid $g_{\alpha,\beta}^{BestEnding}$ of S_n. The $DM_{x,y}^{curr}$ will select the grid $g_{\alpha+\zeta,\beta+\xi}^{k,j,x,y}$ with the largest ζ and the smallest ξ to be the starting grid of S_{n+1}, say $g_{x',y'}^{next}$, for increasing the utilization of directional

Algorithm 1 Basic Approach (BA).

Input: Each directional sensor in R has completed the tasks of *region partitioning* and *coverage identification*. The value k of k-barrier coverage requirement.
Output: A disjoint k-coverage barrier (DB^k)
Initialization: *Initiator* $v_{\hat{1}}$ selection by applying the *initiator competition process.*
// *Best Working Set Construction Process*
$v_i = DM^{curr}_{x,y}$
for all $q^{k,j}_{x,y} \in Q^{k,m}_{x,y}$, where $\forall x_{i,h} = 0,\ v_i \in q^{k,j}_{x,y}$ and $1 \le j \le m$ **do**
  Computes $d(g^{curr}_{x,y}, g^{k,j,x,y}_{\rho,\sigma})$ by applying (8)
$\hat{q}^k_{x,y} = q^{k,j}_{x,y}$ with max. $d(g^{curr}_{x,y}, g^{k,j,x,y}_{\rho,\sigma})$
// *Next Starting Grid Selection Process*
if $\exists v_i \in \hat{q}^k_{x,y}$, where $g_{l,y} \in G_i$ **then**
  return ("*Construction success*")
if $\nexists g^{next}_{x',y'}$ **then**
  return ("*Construction failure*")
$g^{next}_{x',y'} = \max\limits_{\zeta} \min\limits_{\xi} g^{k,j,x,y}_{\alpha+\zeta,\beta+\xi}$
$v_{i'} = DM^{next}_{x',y'}$, where $g^{next}_{x',y'} \in G_{i'}$
$v_i = DM^{prev}_{x,y}$, where v_i is the $DM^{curr}_{x,y}$
for all $v_i \in \hat{q}^k_{x,y}$ **do**
  $x_{i,h} = 1$
Hand_Over($DM^{prev}_{x,y}$, $DM^{next}_{x',y'}$, k)

sensors from top boundary L_{top} to bottom boundary L_{bottom}. That is,

$$g^{next}_{x',y'} = \max_{\zeta} \min_{\xi} g^{k,j,x,y}_{\alpha+\zeta,\beta+\xi}. \tag{10}$$

After $DM^{curr}_{x,y}$ determines the starting grid $g^{next}_{x',y'}$ of S_{n+1}, the $DM^{curr}_{x,y}$ transfers the construction authority to the DM of $g^{next}_{x',y'}$, as denoted by $DM^{next}_{x',y'}$, and changes role from $DM^{curr}_{x,y}$ to *previous* DM, as denoted by $DM^{prev}_{x,y}$. The $DM^{next}_{x',y'}$ will become the role of the *current* DM. That is, the *current* DM of S_{n+1} is $DM^{curr}_{x',y'}$. Executing similar operations done by $DM^{prev}_{x,y}$, the $DM^{curr}_{x',y'}$ will apply the *BA* procedure, including the *best working set construction process* and *next starting grid selection process*, aiming to construct the next segment, until a constructed segment reaches the right boundary W_{right}.

The following continues the example given in Fig. 3 to illustrate the execution of *Next Starting Grid Selection Process*. Recall that the best ending grid of S_1 is $g_{3,2}$. As shown in Fig. 3, the candidate starting grids of S_2 are $g_{4,1}$, $g_{4,2}$, and $g_{4,3}$. By applying (10), the $DM^{curr}_{1,2}$ selects grid $g_{4,1}$, which satisfies the 2-covered restrictions and locates the top-right closest boundary to be the starting grid of segment S_2. As a result, segment S_1 has been constructed and segment S_2 will start to be constructed. The defense barrier will be formed by constructing segment by segment. The *Best Working Set Construction Process* and *Next Starting Grid Selection Process* will be repeatedly applied until a grid of the segment that reaches the right boundary W_{right} is selected, and then the DB^2 is constructed by applying BA mechanism. The pseudo-code of BA is given in Algorithm 1.

The major advantage of BA is simple and easily implemented. However, the BA might be a failure if the $DM^{curr}_{x,y}$ cannot find any next starting grid which satisfies the k-covered restriction. Fig. 4 gives an example that fails to construct a DB^2 by applying BA. Suppose that the segment S_1 between $g_{1,2}$ and $g_{4,2}$ has been constructed as the best working set $\hat{q}^2_{1,2} = \{v_b, v_c\}$ and the $g_{5,1}$ is also selected by $DM^{curr}_{1,2}$ to be the starting grid of segment S_2. Then the $DM^{next}_{5,1}$ takes the construction authority from $DM^{curr}_{1,2}$ and changes role from $DM^{next}_{5,1}$ to $DM^{curr}_{5,1}$. The $DM^{curr}_{5,1}$ further selects $g_{5,1}$ to be the best ending grid of segment S_2 by applying (8) and (9). Note that a grid $g_{x,y}$ can simultaneously play two roles, including starting grid and best ending grid, if $g_{x,y}$ has the largest contribution as compared with all of the other extended grids. Since the $DM^{curr}_{5,1}$ cannot find any grid fully covered by sensing ranges of at least two directional sensors, the BA will fail at $g_{5,1}$ in constructing DB^2. To explore as many as possible feasible solutions, the following presents

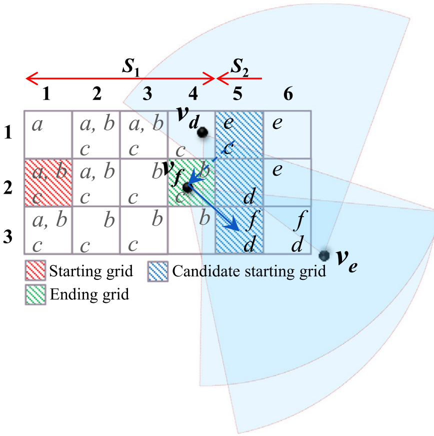

Fig. 4. An example for illustrating the construction of a DB^2 by applying BTA.

a *Backtracking Approach* which can further construct the next segment if the BA fails.

2) Backtracking Approach (BTA)

The basic concept of BTA is to allow the DM^{curr} to transfer the construction authority back to the previous DM, say DM^{prev}, if the DM^{curr} fails to find any grid that satisfies the k-covered restriction. As soon as the DM^{prev} obtains construction authority from DM^{curr}, it plays the role DM^{curr} and tries to find another next starting grid and transfers construction authority to the next new DM. As a result, the construction of DB^k can be continued until a grid of constructed segment reaches the rightmost boundary W_{right}. Thus the BTA provides more opportunities to construct a DB^k rather than BA.

BTA and BA have similar operations if the construction of a DB^k is successful. However, if the $DM^{curr}_{x',y'}$ fails to find the next starting grid which satisfies k-covered restriction from its candidate starting grids $g^{k,j,x',y'}_{\alpha'+\zeta,\beta'+\xi}$, where $-1 \le \zeta \le 1$ and $-1 \le \xi \le 1$, it returns a *construction failure* message to the $DM^{prev}_{x,y}$. Upon receiving the failure message, the $DM^{prev}_{x,y}$ changes role from $DM^{prev}_{x,y}$ to $DM^{curr}_{x,y}$ and tries to select the next starting grid from its candidate starting grids $g^{k,j,x,y}_{\alpha+\zeta,\beta+\xi}$ but omits the grid $g_{x',y'}$. That is,

$$g^{next}_{x',y'} = \max_{\zeta} \min_{\xi} \left(g^{k,j,x,y}_{\alpha+\zeta,\beta+\xi} - g_{x',y'} \right). \tag{11}$$

After that, the $DM^{curr}_{x,y}$ continuously executes a similar procedure as BA and the backtracking mechanism is adopted once the BA fails.

The following continues the example given in Fig. 4 for illustrating the execution of BTA. In Fig. 4, once the $DM^{curr}_{5,1}$ cannot find the k-covered starting grid of segment S_3 from its candidate starting grids, including $g_{6,1}, g_{6,2}, g_{5,1}, g_{5,2}, g_{4,1}$, and $g_{4,2}$, it will transfer the construction authority back to $DM^{prev}_{1,2}$. Upon receiving the construction authority from $DM^{curr}_{5,1}$, the $DM^{prev}_{1,2}$ changes role from $DM^{prev}_{1,2}$ to $DM^{curr}_{1,2}$ and tries to find another starting grid of S_2 from candidate starting grids, including $g_{5,2}, g_{5,3}, g_{4,1}, g_{4,2}, g_{4,3}, g_{3,1}, g_{3,2}$, and $g_{3,3}$. Since grid $g_{5,3}$ satisfies the 2-covered restriction and its contribution calculated by applying (8) is larger than the others except $g_{5,1}$, the $DM^{curr}_{1,2}$ will select grid $g_{5,3}$ as the new starting grid of segment S_2. After taking the construction authority from $DM^{curr}_{1,2}$, the $DM^{next}_{5,3}$ will change its role from $DM^{next}_{5,3}$ into $DM^{curr}_{5,3}$ and will keep on executing the BTA until a constructed segment reaches the boundary W_{right}. The pseudo-code of BTA is given in Algorithm 2.

Although BTA provides more opportunities than BA for successfully constructing a DB^k, only those k-covered grids will be invited

Algorithm 2 Backtracking Approach (BTA).

Input: Each directional sensor in R has completed the tasks of *region partitioning* and *coverage identification*. The value k of k-barrier coverage requirement.
Output: A disjoint k-coverage barrier (DB^k)
Initialization: *Initiator* $v_{\hat{1}}$ selection by applying the *initiator competition process.*

```
if i = DM^{prev}_{x,y} receives "Construction failure" from i' = DM^{curr}_{x',y'} then
    i = DM^{curr}_{x,y}
    g^{next}_{x',y'} = max_ζ min_ξ (g^{k,j,x,y}_{α+ζ,β+ξ} − g_{x',y'})
    v_{i'} = DM^{next}_{x',y'}, where g^{next}_{x',y'} ∈ G_{i'}
    v_i = DM^{prev}_{x,y}, where v_i is the DM^{curr}_{x,y}
    for all v_i ∈ q̂^k_{x,y} do
        x_{i,h} = 1
    Hand_Over(DM^{prev}_{x,y}, DM^{next}_{x',y'}, k)
end if
if receives "Construction success" from Basic Approach then
    return ("Construction success")
else
    return (Basic Approach)
```

6	**4**	**1**
7		**2**
8	**5**	**3**

Fig. 5. Priority table.

to join the construction of DB^k. In fact, those grids that do not satisfy the k-covered restriction can cooperatively contribute to the k-covered grids. The next section, called the Branch Approach, aims to fully utilize those grids that do not satisfy the k-covered restriction.

3) Branch Approach (BRA)

The main idea of BRA is to give more opportunities for the grids which satisfy p-covered but do not satisfy the k-covered restriction, where $p < k$. To accomplish this, the DB^k can be decomposed into several disjoint DB^ps, for $p < k$. These p-covered grids can cooperatively participate in the construction of a DB^k.

Recall that, as shown in (1), a DB^k is a collection of k disjoint DB^1s. In other words, a DB^k can have k branches DB^1_1, DB^1_2, ..., DB^1_{k-1}, and DB^1_k from some grids. Let *weak grid* and *qualified grid* represent the grid whose coverage degrees is less than k and more than or equal to k, respectively. Different from BA and BTA, the BRA can even invite weak grids to participate in the constructed DB^k. Therefore, the BRA can construct more defense barriers than both BA and BTA. Besides, finding more defense barriers can also further balance the workload of directional sensors.

Similar to BA and BTA, the BRA constructs the defense barrier by selecting a qualified grid through grid by grid from W_{right} to W_{left}. However, once the $DM^{curr}_{x,y}$ cannot find the qualified grid as its next starting grid from its candidate starting grids $g^{k,j,x,y}_{\alpha+\zeta,\beta+\xi}$, where $-1 \le \zeta \le 1$ and $-1 \le \xi \le 1$, it initiates the BRA and tries to select some weak grids from the same candidate starting grids $g^{k,j,x,y}_{\alpha+\zeta,\beta+\xi}$ such that the sum of coverage degree of selected weak grids is equal to or larger than k. More specifically, several weak grids in candidate starting grids $g^{k,j,x,y}_{\alpha+\zeta,\beta+\xi}$ will be selected by $DM^{curr}_{x,y}$ to be the next starting grids according to the *priority table* which is described as follows.

The grid selection priority will influence both the number of directional sensors and the chance of successfully constructing a DB^k. As shown in Fig. 5, the priority table is proposed to select appropriately weak grids when the BRA is applied. In Fig. 5, there are 3 × 3 grids. Let the central grid, as marked with slash green line, denote the ending grid of a current constructing segment. The other grids around the ending grid will be the candidate starting grids since each of them can connect to the ending grid. As shown in Fig. 5, a number labeled on each candidate starting grid denotes the selection priority. These numbers are assigned according to the coordinates of these grids. Since the construction of a defense barrier starts from boundary W_{left} and ends at boundary W_{right}, the candidate starting grid located close to the right coordinate means that it is closer to the right boundary W_{right} and hence it has the highest selection priority to play the role of next starting grid than the others. That is, constructing a defense barrier by selecting the starting grid with rightmost coordinates can likely reduce the number of required directional sensors. Furthermore, the candidate grid located close to the top boundary L_{top} also has a higher priority to play the role of the next starting grid than the others because the BRA aims to explore the coverage contribution from all grids from the top grids to the bottom grids.

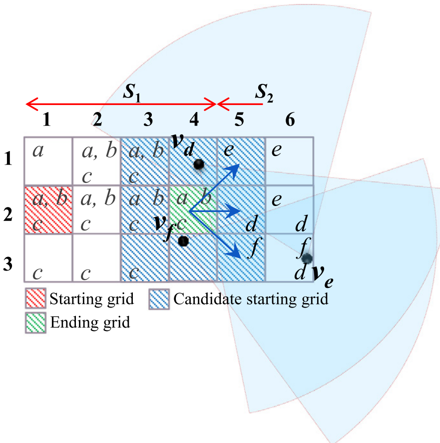

Fig. 6. A running example by applying the BRA.

Fig. 6 depicts an example of how $DM^{curr}_{x,y}$ selects the weak grids according to the priority table for constructing a DB^3. In Fig. 6, assume that the segment S_1, which is composed of those grids starting from grid $g_{1,2}$ to the ending grid $g_{4,2}$, is covered by the best working set $\hat{q}^3_{1,2} = \{v_a, v_b, v_c\}$. However, since the coverage degrees of the candidate starting grids $g_{5,1}$, $g_{5,2}, g_{5,3}$, $g_{4,1}$, $g_{4,2}$, $g_{4,3}$, $g_{3,1}$, $g_{3,2}$, and $g_{3,3}$ are 1, 1, 1, 0, 0, 0, 0, 0, and 0, respectively, none of them satisfies the 3-covered restriction. Consequently, the $DM^{curr}_{1,2}$ initiates the *BRA*. According to the priority table given in Fig. 5, the $DM^{curr}_{1,2}$ selects the grid $g_{5,1}$, which has the highest priority, to be one starting grid. After the grid $g_{5,1}$ is selected for supporting 1-covered, the $DM^{curr}_{1,2}$ will keep selecting another weak grid from the remaining candidate starting grids, including $g_{5,2}$, $g_{5,3}$, $g_{4,1}$, $g_{4,2}$, $g_{4,3}$, $g_{3,1}$, $g_{3,2}$, and $g_{3,3}$, until the sum of the coverage degree achieves the 3-covered restriction. As a result, both the 1-covered grids $g_{5,2}$ and $g_{5,3}$ are subsequently selected by $DM^{curr}_{1,2}$ to be the next starting grids. Through the cooperation of these selected grids $g_{5,1}$, $g_{5,2}$, and $g_{5,3}$, the DB^3 can be constructed by the 1-covered grids $g_{5,1}$, $g_{5,2}$, and $g_{5,3}$.

Let $G = \{g_1, g_2, .., g_\eta\}$ be η weak grids selected by $DM^{curr}_{x,y}$. Let c_ω denote the coverage degree of grid g_ω, where $g_\omega \in G$. To guarantee that the η branches can cooperatively support the k-covered restriction, the η weak grids selected by $DM^{curr}_{x,y}$ should satisfy (12).

$$\sum_{\omega=1}^{\eta} c_\omega \ge k \tag{12}$$

The next step is that each DM of g_ω, also called DM^{next}, further takes the construction authority from DM^{curr} and plays the role of DM^{curr}, aiming to further construct the next segment with coverage degree c_ω. During segment construction, if the DM^{curr}

Algorithm 3 Branch Approach (BRA).

Input: Each directional sensor in R has completed the tasks of *region partitioning* and *coverage identification*. The value k of k-barrier coverage requirement.
Output: A disjoint k-coverage barrier (DB^k)
Initialization: *Initiator* $v_{\hat{1}}$ selection by applying the *initiator competition process*.

if receives "*Construction failure*" **then**
  while $c_\omega \le k$, where $1 \le \omega \le \eta$ **do**
    Select $g^{next}_{x',y'}$ based on *Priority Table*
    $v_{i'} = DM^{next}_{x',y'}$, where $g^{next}_{x',y'} \in G_{i'}$
    $v_i = DM^{prev}_{x,y}$, where v_i is the $DM^{curr}_{x,y}$
    for all $v_i \in \hat{q}^k_{x,y}$ **do**
      $x_{i,h} = 1$
    Hand_Over($DM^{prev}_{x,y}$, $DM^{next}_{x',y'}$, k)
end if
if receives "*Construction success*" from *Basic Approach* **then**
  return ("*Construction success*")
else
  return (*Basic Approach*)

of g_ω encounters the situation that all of the candidate starting grids cannot support the k-covered restriction, it further applies the BRA to branch the current segment into several segments with smaller coverage degree. The segment construction will be continuously executed until all of the branched segments reach the rightmost boundary W_{right}. Recall that with the *sensor-disjoin constraint* given in (6), different defense barriers cannot share the common directional sensor. Therefore, when the BRA is applied, the branched segments cannot share the common directional sensor. The pseudo-code of BRA is given in Algorithm 3.

The following continues the example given in Fig. 6 for illustrating the execution of BRA after the $DM^{curr}_{1,2}$ determines the weak grids $g_{5,1}$, $g_{5,2}$, and $g_{5,3}$. In Fig. 6, the $DM^{curr}_{5,3}$ transfers the construction authorities to the DMs: $DM^{next}_{5,1}$, $DM^{next}_{5,2}$, and $DM^{next}_{5,3}$. Upon receiving the construction authorities, these DMs change their role from $DM^{next}_{5,1}$, $DM^{next}_{5,2}$, and $DM^{next}_{5,3}$ into $DM^{curr}_{5,1}$, $DM^{curr}_{5,2}$, and $DM^{curr}_{5,3}$, respectively. Then, the DMs, including $DM^{curr}_{5,1}$, $DM^{curr}_{5,2}$, and $DM^{curr}_{5,3}$, individually apply the BRA to construct the defense barrier with coverage degrees 1, 1, and 1, respectively. As a result, the DB^3 is accomplished if all of the branches DB^1s reach the rightmost boundary W_{right}.

5. Analyses of *k*-BCC

This section analyzes the message complexity and the efficiency of the proposed mechanism $k-$BCC.

5.1. Analysis of message complexity

When executing the proposed k-BCC mechanism, two types of messages, including the *Hello* message and the *Construction* message, should be used. Each sensor only needs to exchange a *Hello* message with its neighbors once. The Hello message is mainly composed of the ID and coordinates of the transmitter, and the coordinates of grids that can be fully covered by the transmitter. Let notation q denote the average number of neighboring sensors. The message complexity of each sensor requires $\mathcal{O}(q)$ in terms of the number of *Hello* message exchanges. Consequently, the message complexity of whole sensor network requires $\mathcal{O}(qn)$ for the number of Hello message exchanges. Based on the received Hello message, each sensor can make a decision whether or not it should play the role of decision maker. The other message is called *Construction* message which is exchanged by DMs. The *Construction* message is composed of the transmitter's ID, receivers' IDs, and the required k-coverage degree. The sensor that plays the role of DM will further transmit the *Construction* messages to its neighboring sensors, aiming to construct a segment of a defense k-coverage barrier. The defense k-coverage barrier will be constructed segment by segment while the Construction messages are exchanged between neighboring sensors from leftmost to rightmost boundaries. Let notation $\hbar$ denote the number of DMs. The value of $\hbar$ will be the same with the total number of grids in a given region. Therefore, the message complexity of the *Construction* message requires $\mathcal{O}(\hbar^2)$.

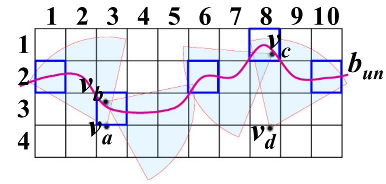

Fig. 7. An example that k-BCC misses to construct the existed defense barrier b_{un}.

5.2. Analysis of efficiency

Recall that the k-BCC constructs a DB^k by using the concept of a grid-based region which simplifies the k-barrier coverage problem for reducing the computational complexity. However, adopting a grid-based concept may mean losing opportunities to construct more defense barriers, as compared with the brute-force algorithm. Let *undiscovered defense barrier*, denoted by b_{un}, represent the existing defense barrier that is unable to be constructed by the proposed k-BCC mechanism. Fig. 7 depicts an example of the b_{un}. In Fig. 7, some grids, such as $g_{1,2}$, $g_{3,3}$, $g_{6,2}$, $g_{8,1}$, and $g_{10,2}$, are not *fully covered grids* as defined in the previous definition. The corresponding directional sensors v_a, v_b, v_c, and v_d will ignore them and hence the proposed k-BCC mechanism is unable to construct the defense barrier b_{un}. From this example, it is obvious that adopting the grid-based concept will discard some existing defense barriers, reducing the defense efficiency. This section aims to analyze the probability that a defense barrier exists in the region, but it is unable to be constructed by the proposed k-BCC mechanism.

Let *fully covered grid* $g^{fully}_{i,x,y}$, *partially covered grid* $g^{partial}_{i,x,y}$ and *emptily* covered *grid* $g^{empty}_{i,x,y}$ denote the grid $g_{x,y}$ that is fully, partially and emptily covered by directional sensor v_i, respectively. As shown in Fig. 7, the grids $g_{2,2}$ and $g_{3,1}$ are fully covered and partially covered by v_a, respectively. Hence the grids $g_{2,2}$ and $g_{3,1}$ can be represented by $g^{fully}_{a,2,2}$ and $g^{partial}_{a,3,1}$, respectively. On the other hand, the grid $g_{4,1}$ can be represented by $g^{empty}_{t,4,1}$, where $t \in \{v_a, v_b, v_c, v_d\}$, because that grid $g_{4,1}$ is not covered by any directional sensor.

A grid $g_{x,y}$ is said to be *connectedly partial covered grid*, denoted by $g^{conn}_{i,j,x,y}$, if it is partially covered by both directional sensors v_i and v_j, and the sensing ranges of v_i and v_j overlap in $g_{x,y}$. In particular, a grid $g_{x,y}$ is said to be *boundary connectedly partial covered grid*, denoted by $g^{bconn}_{i,x,y}$, if we treat left boundary W_{left} or right boundary W_{right} as the sensing range of a virtual sensor v_j and the grid $g_{x,y}$ still satisfies *connectedly partial covered grid*. As shown in Fig. 7, grid $g_{3,3}$ can be represented by $g^{conn}_{a,b,3,3}$ or $g^{conn}_{b,a,3,3}$. On the other hand, grids $g_{1,2}$ and $g_{10,2}$ can be represented by $g^{bconn}_{a,1,2}$ and $g^{bconn}_{d,10,2}$, respectively.

Since both $g^{conn}_{i,j,x,y}$ and $g^{bconn}_{i,x,y}$ will be ignored by applying the proposed mechanism $k-$BCC, the *undiscovered defense barrier* b_{un} may exist. As shown in Fig. 7, the defense barrier b_{un} consisting of $g^{bconn}_{a,1,2}$, $g^{bconn}_{d,10,2}$, $g^{conn}_{a,b,3,3}$, $g^{conn}_{b,c,6,2}$, and $g^{conn}_{c,d,8,1}$ exists but it cannot be constructed by the proposed k-BCC. Let P^{lose} denote the probability of existing b_{un}. The following evaluates the value of P^{lose}.

1) The Evaluation of P^{lose}

This section evaluates the value of P^{lose}. Recall that the undiscovered defense barrier b_{un} only happens when there exists a

$g^{conn}_{i,j,x,y}$ or $g^{bconn}_{i,x,y}$ in DB^1. Let $p^{conn}_{i,j,x,y}$ or $p^{bconn}_{i,x,y}$ denote the probabilities of a $g^{conn}_{i,j,x,y}$ or $g^{bconn}_{i,x,y}$ existing, respectively. The value of P^{lose} varies with the values of $p^{conn}_{i,j,x,y}$ or $p^{bconn}_{i,x,y}$. The following firstly evaluates the value of $p^{conn}_{i,j,x,y}$. Then the value of $p^{bconn}_{i,x,y}$ is evaluated. Based on the evaluations of $p^{conn}_{i,j,x,y}$ and $p^{bconn}_{i,x,y}$, the P^{lose} can be derived in the end of this section.

a. Evaluation of $\boldsymbol{p^{conn}_{i,j,x,y}}$

Assume that there are n^{empty} grids uncovered by any directional sensor in the given monitored region R. Recall that the number of directional sensors deployed in R is denoted by notation n. Since the n^{empty} uncovered grids are not covered by any directional sensor, on the average, the number of uncovered grids neighboring each directional sensor is measured by n^{empty}/n, denoted by n^{empty}_{avg}. As shown in Fig. 7, each of the directional sensors, including v_a, v_b, v_c, and v_d, has $n^{empty}_{avg} = 5/4$ average uncovered grids.

Let n^{full}_{avg} and $n^{partial}_{avg}$ respectively denote the average number of fully and partially covered grids for each directional sensor. Let n^{duty}_{each} denote the summation of n^{full}_{avg}, $n^{partial}_{avg}$, and n^{empty}_{avg}, as depicted in (13).

$$n^{duty}_{each} = n^{full}_{avg} + n^{partial}_{avg} + n^{empty}_{avg} \tag{13}$$

Furthermore, let notations p^{full}_{each}, $p^{partial}_{each}$, and p^{empty}_{each} denote the probabilities that there would exist a fully covered grid, partially covered grid and emptily covered grid for each directional sensor, respectively. The probabilities p^{full}_{each}, $p^{partial}_{each}$, and p^{empty}_{each} satisfy (14).

$$p^{full}_{each} + p^{partial}_{each} + p^{empty}_{each} = \frac{n^{full}_{avg}}{n^{duty}_{each}} + \frac{n^{partial}_{avg}}{n^{duty}_{each}} + \frac{n^{empty}_{avg}}{n^{duty}_{each}} = 1 \tag{14}$$

The probabilities p^{full}_{each}, $p^{partial}_{each}$ and p^{empty}_{each} can be used to estimate the probabilities of a fully covered grid, partially covered grid and emptily covered grid existing between two neighboring directional sensors, as shown in (15).

$$\begin{aligned}&\left(p^{full}_{each} + p^{partial}_{each} + p^{empty}_{each}\right)^2\\ &= \left(p^{full}_{each}\right)^2 + \left(p^{partial}_{each}\right)^2 + \left(p^{empty}_{each}\right)^2 + 2\cdot p^{full}_{each}\cdot p^{partial}_{each}\\ &\quad + 2\cdot p^{partial}_{each}\cdot p^{empty}_{each} + 2\cdot p^{full}_{each}\cdot p^{empty}_{each}\end{aligned} \tag{15}$$

In (15), the term $(p^{partial}_{each})^2$ means the probability of a grid which is partially covered by two neighboring directional sensors simultaneously while the term $(2\cdot p^{full}_{each}\cdot p^{partial}_{each})$ represents the probability of a grid that is fully covered by a directional sensor but partially covered by another.

Let $g^{aconn}_{i,j,x,y}$ denote the grid $g_{x,y}$ that is not ignored by applying the k-BCC but still satisfies the two conditions 1) the $g_{x,y}$ is covered by v_i and v_j, 2) the sensing ranges of v_i and v_j are overlapped in $g_{x,y}$. Let $p^{aconn}_{i,j,x,y}$ denote the probability that there exists a $g^{aconn}_{i,j,x,y}$. According to (15), the $p^{aconn}_{i,j,x,y}$ can be evaluated by applying (16).

$$p^{aconn}_{i,j,x,y} = \left(p^{full}_{each}\right)^2 + 2\cdot p^{full}_{each}\cdot p^{partial}_{each} \tag{16}$$

Recall that the *connectedly partial covered gird* $g^{conn}_{i,j,x,y}$ is the grid $g_{x,y}$ that is partially covered by v_i and v_j, and their sensing ranges overlap in $g_{x,y}$. Since a grid partially covered by two directional sensors might be connected or not connected, the $p^{conn}_{i,j,x,y}$ can be evaluated by applying (17).

$$p^{conn}_{i,j,x,y} = \left(p^{partial}_{each}\right)^2/2 \tag{17}$$

In addition to the derivation of the value of $p^{conn}_{i,j,x,y}$, the evaluation of P^{lose} value still needs to evaluate the value of $p^{bconn}_{i,x,y}$. The following paragraph presents the derivation of $p^{bconn}_{i,x,y}$.

b. Evaluation of $\boldsymbol{p^{bconn}_{i,x,y}}$

The following evaluates the $p^{bconn}_{i,x,y}$. Recall that the considered monitoring region is $R = L\times W$. The grid size is denoted by $l\times l$. Let Φ denote the total number of partitioned grids in R. The value of Φ can be calculated by applying (18).

$$\Phi = \lceil L/l\rceil\cdot\lceil W/l\rceil \tag{18}$$

Let $p^{boun}_{x,y}$ denote the probability of a grid $g_{x,y}$ existing that is adjacent to the boundaries W_{left} or W_{right}. According to (18), the value of $p^{boun}_{x,y}$ can be estimated by applying (19).

$$p^{boun}_{x,y} = 2\cdot\lceil W/l\rceil/\Phi = 2/\lceil L/l\rceil \tag{19}$$

Let $g^{abconn}_{i,x,y}$ denote the grid $g_{x,y}$ that is not ignored by applying the k-BCC but still satisfies the three conditions 1) the $g_{x,y}$ is adjacent to the boundaries W_{left} or W_{right}, 2) the $g_{x,y}$ is covered by v_i, 3) the sensing range of v_i intersects with the boundaries W_{left} or W_{right}. Let $p^{abconn}_{i,x,y}$ denote the probability of a $g^{abconn}_{i,x,y}$ existing. According to (15), the $p^{abconn}_{i,x,y}$ can be evaluated by applying (20).

$$p^{abconn}_{i,x,y} = p^{boun.}_{x,y}\cdot p^{full}_{each} \tag{20}$$

Similar to (17), consider a grid $g_{x,y}$ that is partially covered by v_i. It is obvious that the sensing range of v_i might connect or not connect to any boundary (W_{left} or W_{right}). According to (15), the value of $p^{bconn}_{i,x,y}$ can be calculated by applying (21).

$$p^{bconn}_{i,x,y} = (p^{boun}_{x,y}\cdot p^{partial}_{each})/2 = p^{partial}_{each}/\lceil L/l\rceil. \tag{21}$$

c. Evaluation of $\boldsymbol{P^{lose}}$

According to (16), (17), (20), and (21), the following further presents the evaluation of P^{lose}. Recall that the *undiscovered defense barrier* b_{un} would occur if the constructing DB^1 contains either $g^{conn}_{i,j,x,y}$ or $g^{bconn}_{i,x,y}$. Let notation m_B denote the required average number of directional sensors for constructing a DB^1 by applying the k-BCC. In the worst case, suppose b_{un} occurs. That is to say that the b_{un} has either (m_B-1) independent chances for containing at least one $g^{conn}_{i,j,x,y}$, or 2 independent chances for containing at least one $g^{bconn}_{i,x,y}$.

The following gives an example to help understand the above-mentioned concept. As show in Fig. 7, the number of directional sensors for constructing DB^1, which is composed of v_a, v_b, v_c, and v_d, is $m_B = 4$. Consequently, there are $(m_B-1) = 3$ independent chances for containing at least one $g^{conn}_{i,j,x,y}$ formed by $\{v_a, v_b\}$, $\{v_b, v_c\}$, or $\{v_c, v_d\}$. Also, there are 2 independent chances for containing at least one $g^{bconn}_{i,x,y}$ formed by $\{W_{left}, v_a\}$ or $\{v_d, W_{right}\}$.

Therefore, the composition of P^{lose} can be divided into three possible cases. Let notations p_1, p_2 and p_3 be the probabilities of the three cases. The first case is that the constructing DB^1 contains at least one $g^{conn}_{i,j,x,y}$ with (m_B-1) independent chances and does not contain $g^{bconn}_{i,x,y}$ with 2 independent chances. According to (16), (17), and (20), the p_1 can be evaluated by applying (22).

$$p_1 = \left(p^{abconn}_{i,x,y}\right)^2\cdot\sum_{u=1}^{m_B-1}\binom{m_B-1}{u}\cdot\left(p^{conn}_{i,j,x,y}\right)^u\cdot\left(p^{aconn}_{i,j,x,y}\right)^{m_B-1-u} \tag{22}$$

In the second case, two conditions should be satisfied. First, the constructing DB^1 does not contain $g^{conn}_{i,j,x,y}$ that has (m_B-1) independent chances. The second condition is that there contains at least one $g^{bconn}_{i,x,y}$ with 2 independent chances. According to (16), (20), and (21), the probability of the second case, denoted by p_2, can be evaluated by applying (23).

$$p_2 = \left(p^{aconn}_{i,j,x,y}\right)^{m_B-1}\cdot\sum_{u=1}^{2}\binom{2}{u}\cdot\left(p^{bconn}_{i,x,y}\right)^u\cdot\left(p^{abconn}_{i,x,y}\right)^{2-u} \tag{23}$$

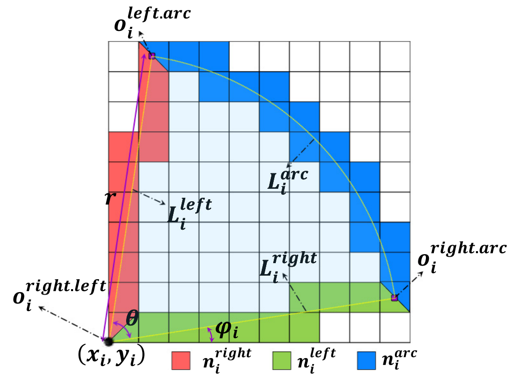

Fig. 8. The calculation of the number of partially covered grids of v_i.

The last case is that the constructing DB^1 contains at least one $g^{conn}_{i,j,x,y}$ with (m_B-1) independent chances and at least one $g^{bconn}_{i,x,y}$ with 2 independent chances. According to (13), (17), (20), and (21), the probability of the last case, denoted by p_3, can be evaluated by applying (24).

$$p_3 = \left[\sum_{u=1}^{m_B-1}\binom{m_B-1}{u}\cdot\left(p^{conn}_{i,j,x,y}\right)^u\cdot\left(p^{aconn}_{i,j,x,y}\right)^{m_B-1-u}\right] \times \left[\sum_{u=1}^{2}\binom{2}{u}\cdot\left(p^{bconn}_{i,x,y}\right)^u\cdot\left(p^{abconn}_{i,x,y}\right)^{2-u}\right] \quad (24)$$

Based on (22)–(24), the P^{lose} can be estimated by applying (25).

$$P^{lose} = \sum_{u=1}^{3} p_u \quad (25)$$

2) The Evaluations of $\boldsymbol{n^{full}_{avg}}$ and $\boldsymbol{n^{partial}_{avg}}$

This section aims to evaluate both the average number of fully covered grids n^{full}_{avg} and partially covered grids $n^{partial}_{avg}$ in detail. As shown in (13)–(25), the value of P^{lose} varies with both the n^{full}_{avg} and $n^{partial}_{avg}$. Recall the assumptions that a directional sensor v_i has a non-rotatable *sensing range* with sensing range r, field-of-view (FoV) angle θ_i, and orientation vector ϕ_i, as shown in Fig. 8. Both the n^{full}_{avg} and $n^{partial}_{avg}$ are impacted by r, θ_i, and ϕ_i. The following firstly presents the evaluation of $n^{partial}_{avg}$.

As shown in Fig. 8, let notations L_i^{right}, L_i^{left}, and L_i^{arc} denote the *right coverage boundary, left coverage boundary*, and *arc coverage boundary* of v_i with θ_i, r, and ϕ_i, respectively. Let notations n_i^{right}, n_i^{left}, and n_i^{arc} denote the numbers of partially covered grids covered by L_i^{right}, L_i^{left}, and L_i^{arc}, respectively. The total number of partially covered grids covered by v_i, denoted by $n_i^{partial}$, can be evaluated by applying (26).

$$n_i^{partial} = n_i^{right} + n_i^{arc} + n_i^{left} - 3 \quad (26)$$

The following explains (26) in detail. A movement is said to be valid if it moves along either the positive x-axis direction or the positive y-axis direction. Each shortest path moving from source point (x_s,y_s) to terminal point (x_t,y_t) requires (x_t-x_s) movements in x-axis and (y_t-y_s) movements in y-axis, where $x_s \le x_t$ and $y_s \le y_t$. Recall that the size of a grid is $l \times l$. As shown in Fig. 8, let $o_i^{right.left} = (x_i, y_i)$, $o_i^{right.arc} = (x_i + r\cos\varphi_i, y_i + r\sin\varphi_i)$, and $o_i^{left.arc} = (x_i + r\cos(\varphi_i+\theta_i), y_i + r\sin(\varphi_i+\theta_i))$ denote the *connection points* between L_i^{right} and L_i^{left}, L_i^{right} and L_i^{arc}, and L_i^{left} and L_i^{arc}, respectively. Obviously, the edge L_i^{right} is a *shortest path* from $o_i^{right.left}$ to $o_i^{right.arc}$. Therefore, the number of partially covered grids covered by L_i^{right}, say n_i^{right}, can be evaluated by

Table 3
Estimations of P^{lose}.

l	n^{full}_{avg}	$n^{partial}_{avg}$	n^{empty}_{avg}	P^{lose}
8 m	2.67	4.53	1.28	1.83%
4 m	14.82	8.62	14.47	0.98%
2 m	68.71	18.78	63.27	0.46%
1 m	297.87	40.26	283.78	0.18%

$$n_i^{right} = \left\lceil \overline{o_i^{right.left}o_i^{right.arc}}/l \right\rceil + 1 = \left\lceil \sqrt{(r\cos\varphi_i)^2 + (r\sin\varphi_i)^2}/l \right\rceil + 1. \quad (27)$$

Similar to n_i^{right}, n_i^{arc} and n_i^{left} can also be evaluated by applying (28) and (29), respectively.

$$n_i^{arc} = 1 + \left\lceil \overline{o_i^{right.arc}o_i^{left.arc}}/l \right\rceil = 1 + \left\lceil \sqrt{[r\cos(\varphi_i+\theta_i) - r\cos\varphi_i]^2 + [r\sin(\varphi_i+\theta_i) - r\sin\varphi_i]^2}/l \right\rceil \quad (28)$$

$$n_i^{left} = 1 + \left\lceil \overline{o_i^{right.left}o_i^{left.arc}}/l \right\rceil = 1 + \left\lceil \sqrt{[r\cos(\varphi_i+\theta_i)]^2 + [r\sin(\varphi_i+\theta_i)]^2}/l \right\rceil \quad (29)$$

According to (27)–(29), the total number of partially covered grids that are covered by v_i, say $n_i^{partial}$, can be further derived as

$$\begin{aligned} n_i^{partial} &= \left\lceil \overline{o_i^{right.left}o_i^{right.arc}}/l \right\rceil + \left\lceil \overline{o_i^{right.arc}o_i^{left.arc}}/l \right\rceil + \left\lceil \overline{o_i^{right.left}o_i^{left.arc}}/l \right\rceil = \left\lceil \sqrt{(r\cos\varphi_i)^2 + (r\sin\varphi_i)^2}/l \right\rceil \\ &+ \left\lceil \sqrt{[r\cos(\varphi_i+\theta_i) - r\cos\varphi_i]^2 + [r\sin(\varphi_i+\theta_i) - r\sin\varphi_i]^2}/l \right\rceil \\ &+ \left\lceil \sqrt{[r\cos(\varphi_i+\theta_i)]^2 + [r\sin(\varphi_i+\theta_i)]^2}/l \right\rceil. \end{aligned} \quad (30)$$

Finally, consider that the orientation vector ϕ_i also impacts each $n_i^{partial}$, the average number of fully covered grids, say $n^{partial}_{avg}$, can be derived by applying (31).

$$n^{partial}_{avg} = \sum_{u=1}^{2\pi/\theta_i} \left(n_i^{partial}\right)_u / (2\pi/\theta_i) \quad (31)$$

The following presents the evaluation of n^{full}_{avg}. To evaluate the value of n^{full}_{avg}, let n_i^{full} denote the total number of fully covered grids covered by v_i. As shown in Fig. 8, the value of n_i^{full} can be evaluated by applying (32).

$$n_i^{fully} = \sum_{u=1}^{\lfloor r/l \rfloor} \lfloor (u \cdot l \cdot tan\theta_i)/l \rfloor \quad (32)$$

Similarly, the value of n^{full}_{avg} can be calculated by applying (33).

$$n^{full}_{avg} = \left[\sum_{u_2=1}^{\lfloor 2\pi/\theta_i \rfloor} \sum_{u_1=1}^{\lfloor r/l \rfloor} \lfloor (u \cdot l \cdot tan\theta_i)/l \rfloor \right] / (2\pi/\theta_i) \quad (33)$$

In summary, the P^{lose} increases with $p^{conn}_{i,j,x,y}$ and $p^{bconn}_{i,x,y}$. On the other hand, $p^{conn}_{i,j,x,y}$ and $p^{bconn}_{i,x,y}$ increase with $n^{partial}_{avg}$ and decrease with the n^{full}_{avg}. Table 3 depicts the estimations of P^{lose} values based on (25), where $R = 400$ m × 400 m, $r = 20m$, $\theta_i = \pi/2$, $\phi_i = \pi/12$, $|V| = 600$, and $m_B = 23$. Table 3 reflects the fact that the increased

Table 4
Simulation parameters.

Monitored region	400 m × 400m
Number of directional sensors	300–600
Grid size	1 m, 2 m, 4 m, 8m
Sensing radius	5m–30m
Comm. radius	2 × Sensing radius (r)
FoV	0.5(rad)–2(rad)
Deployment	Random

magnitude of n_{avg}^{full} is much larger than $n_{avg}^{partial}$. This also indicates that the value of P^{lose} will remain very small even if the $n_{avg}^{partial}$ increases. The next section will further investigate the approximate value of P^{lose} based on extensive experiments.

6. Simulation

This section shows the performance comparisons of BA, BTA, BRA, and Maximum Disjoint Paths (MDP) mechanism. The MDP mechanism proposed in [23] is a centralized method which applies exhausted search on the possible solutions. Therefore, we treat the MDP as the optimal solution. We also compare the performance of the proposed k-BCC and the existing distributed algorithms CoBRA [17] and D-TriB [19]. In CoBRA, the main idea is that the contribution of the sensing range of each directional sensor is transformed into a partial barrier line. A set of partial barrier lines are selected by several directional sensors based on their coordinates and lengths. Similar to CoBRA, the D-TriB initially converts the FoV of each directional sensor into a horizontal line. After this, a directional sensor located at the leftmost boundary is selected to be the initiator. Based on the horizontal line of each directional sensor, the initiator selects suitable relay directional sensors from left to right until the leftmost boundary is reached and the defense 1-barrier is completed. We further compare the performances of the proposed k-BCC and the Max-Num-Barrier-Greedy (MNBG) algorithm proposed by [21]. In MNBG, the given region is firstly transformed into a weighted graph. Later on, the MNBG finds the shortest path from leftmost to rightmost boundaries on the weighted graph using Dijkstra's algorithm until no path can be found. Each found shortest path is considered as a defense 1-coverage barrier. We evaluate the performances of the proposed k-BCC in a discrete event network simulator ns-3.26. A set of directional sensors ranging from 300 to 600 is randomly deployed in a 400 m × 400 m monitoring area. The communication radius is twice the sensing radius ranging from 5 m to 30 m. The grid size is set by 1 m, 2 m, 4 m, and 8 m. The FoV is set ranging from 0.5(rad)–2(rad). The simulation parameters are given in Table 4. Fig. 9 gives a snapshot of our simulation environment.

Similar to the proposed k-BCC, two types of messages, such as *Hello* message and *Construction* message, are used for CoBRA [17] and D-TriB [19] aiming to construct a barrier. The basic concept of their algorithms is that each sensor firstly collects the local information of its neighbors by exchanging the *Hello* message. The complexity of *Hello* message exchanges requires $\mathcal{O}(qn)$ for the whole sensor network, which is equivalent to the k-BCC. Based on the received Hello message, the contribution of each sensor on barrier is transformed into a partial barrier line. The set of sensors that contribute to the largest partial barrier line will be selected. The length of the partial barrier line can be enlarged if two partial barrier lines overlap. As a result, a defense 1-coverage barrier can be constructed from the leftmost to the rightmost boundaries. Since both the CoBRA [17] and D-TriB [19] only consider constructing the defense 1-coverage barrier, the message complexity of the *Construction* message requires $\mathcal{O}(n^2k)$ in terms of k-barrier coverage. Therefore, their control message overhead is $\mathcal{O}(n^2k/\hbar)$ times higher than the proposed k-BCC.

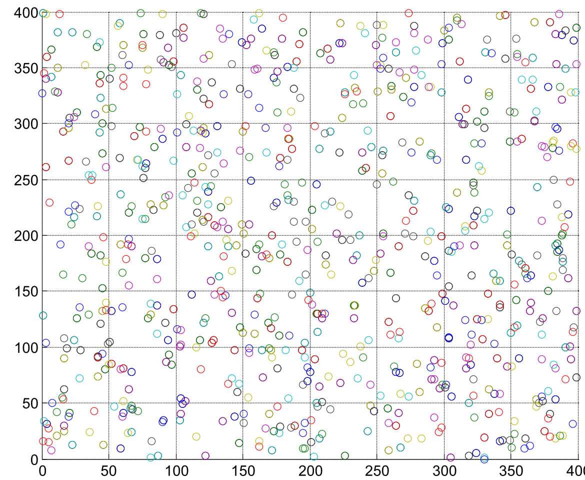

Fig. 9. A snapshot of the simulation environment.

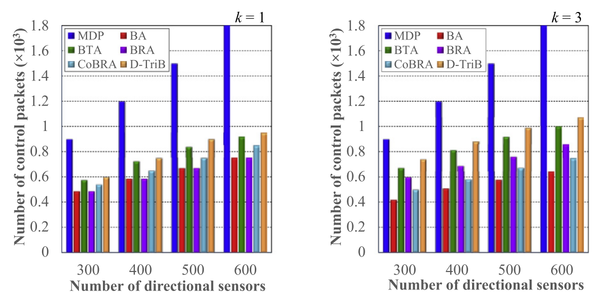

(a) 1-Barrier coverage. (b) 3-Barrier coverage.

Fig. 10. Performance comparison of BA, BTA, BRA, CoBRA, D-TriB, and MDP in terms of control overheads with different number of directional sensors. The cover requirement is k-barrier coverage. The R and r are set by R = 400 m × 400 m, and r = 20m, respectively.

Fig. 10 investigates the control overhead of MDP, CoBRA, D-TriB, and the proposed BA, BTA, and BRA algorithms by varying the number of directional sensors under different requirement of DB^k. Fig. 10(a) compares the number of control packets when the number of directional sensors is ranging from 300 to 600 under the requirement of 1-barrier coverage. As shown in Fig. 10(a), the proposed BA, BTA, and BRA outperform the optimal solution MDP. This occurs because the MDP is a centralized algorithm and it needs to collect information and to broadcast the results between the sink and all the directional sensors. In contrast, the main control overheads of BA, BRA, and BTA only occur between DM^{curr} and its neighbors. Moreover, since the cover requirement is 1-barrier coverage, there is no *weak grid* and thus the solution space can be significantly reduced. This helps reduce the control overhead. As shown in Fig. 10(a), both BRA and BA create the same number of control packets. On the other hand, the proposed BTA creates a larger number of control packets than BA and BRA. This occurs because the BTA can still adopt the detour policy to find more possible solutions when $k = 1$. Moreover, since both of the existing works CoBRA and D-TriB require high-precision calculations and more control packet exchanges for identifying the connection relation between two directional sensors, the proposed BA and BRA outperform the existing CoBRA and D-TriB.

Fig. 10(b) further investigates the number of control packets when $k = 3$. Similarly, the proposed BA, BTA, and BRA outperform the MDP. Besides, the BRA creates more control overhead than BA. The results of Fig. 10(a) and (b) are different if we compare the

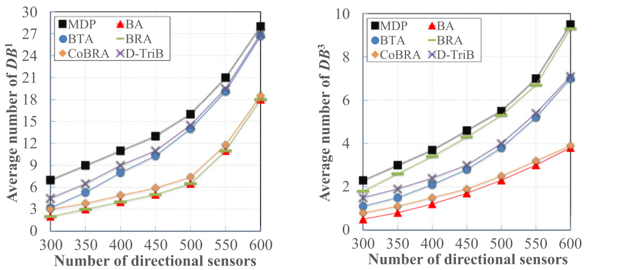

(a) 1-Barrier coverage. (b) 3-Barrier coverage.

Fig. 11. Performance comparison of BA, BTA, BRA, CoBRA, D-TriB, and MDP in terms of average number of DB^k by varying the number of directional sensors. The R, l, and r are set by $R = 400\text{m} \times 400\text{m}$, $l = 1\text{m}$, and $r = 20\text{m}$, respectively.

BRA and BA mechanisms. Recall that the control overheads of BRA and BA are identical in Fig. 10(a). The result of Fig. 10(b) is different from that of Fig. 10(a). This occurs because the BRA can explore more possible solutions by considering the 1-*covered* weak grids when it aims to construct additional DB^3. In contrast, the BA will encounter the dead-end problem earlier than the BRA, which causes the control overhead of BA to be lower than that of BRA. In addition, since the BRA further invites more weak grids to participate in the construction of DB^3, it can construct more DB^3 than CoBRA. This also means that the BRA requires more control packet exchanges than CoBRA.

Given a fixed number of directional sensors ranging from 300 to 600, Fig. 11 investigates the average number of DB^k, where $1 \le k \le 4$, by applying BA, BTA, BRA, MDP, CoBRA, and D-TriB. As shown in Fig. 11(a), MDP outperforms BA, BTA, BRA, CoBRA, and D-TriB in terms of average number of DB^1. This occurs because the MDP firstly calculates all of the possible DB^1 solutions, and then selects the one which consists of the smallest number of directional sensors. However, as observed in Fig. 10, the MDP creates significant control overhead than the proposed BA, BTA, and BRA. Compared to this, Fig. 11(a) also shows that the BRA equals the BA in terms of the average number of DB^1. This occurs because there is no weak grid existing in the given monitored region if $k = 1$. Therefore, the BRA will degenerate to BA when $k = 1$. Moreover, since the BTA can still adopt the detour policy when encountering the dead-end problem, the BTA outperforms BA and BRA. As mentioned in Section 5, since the value of P^{lose} keeps a very small value, the performances of BTA and CoBRA are similar. In addition, the performances of BA and BRA are very close to that of D-TriB.

Fig. 11(b) further investigates the average number of DB^3 by applying BA, BTA, BRA, CoBRA, D-TriB, and MDP. As shown in Fig. 11(b), the BRA outperforms the BA, BTA, CoBRA, and D-TriB in terms of average number of DB^3. This occurs because the BRA can further consider 1-covered weak grids and hence it can explore more solutions for constructing DB^3 when encountering the dead-end problem. In addition, the numbers of DB^3 constructed by applying BRA and MDP are approximate.

Fig. 12 investigates the value of P^{lose} by varying the grid size ranging from 1 m to 8 m. Four curves, denoted by $P^{lose}(\pi/4)$, $P^{lose}(\pi/2)$, $P^{lose}(2\pi/3)$, and $P^{lose}(\pi)$, which apply different FoVs, including $\pi/4$, $\pi/2$, $2\pi/3$, and π, are compared in terms of the value of P^{lose}. In general, the value of P^{lose} of four curves increases with the size of the grid. A large grid size increases the value of $n_{avg}^{partial}$, which leads to a large value of P^{lose}. When the grid size drops, the increasing magnitudes of n_{avg}^{full} and n_{avg}^{empty} are much larger than that of $n_{avg}^{partial}$. Thus, the value of P^{lose} significantly drops. In general, the $P^{lose}(\pi)$ outperforms the $P^{lose}(2\pi/3)$, $P^{lose}(\pi/2)$, and $P^{lose}(\pi/4)$ in terms of the value of P^{lose}. This occurs because the FoV with angle π covers more *fully covered grids* than the others.

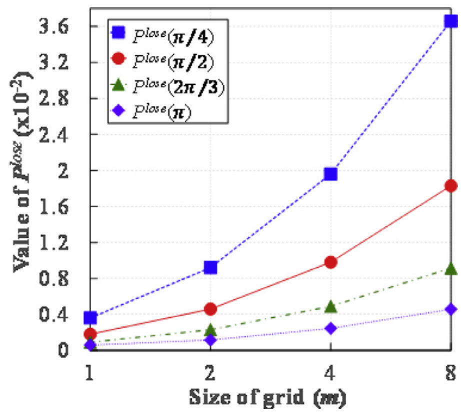

Fig. 12. Performance evaluation on P^{lose} with different FoV including $\pi/4$, $\pi/2$, $2\pi/3$, and π by varying the size of grid ranging from 1 m to 8 m in a fixed region $R = 400\text{m} \times 400\text{m}$, where $|V| = 600$ and $r = 20\text{m}$.

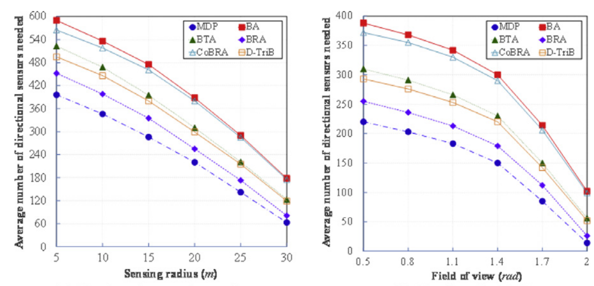

(a) Varying the sensing radius. (b) Varying the FoV.

Fig. 13. Performance comparison of BA, BTA, BRA, CoBRA, D-TriB and MDP in terms of average number of directional sensors needed for constructing a DB^3 by (a) varying the sensing radius and (b) varying the FoV. The R, l, and FoV are set by $R = 400\text{m} \times 400\text{m}$, $l = 1\text{m}$, and FoV $= \pi/2$, respectively.

Fig. 13(a) investigates the average number of directional sensors needed for constructing a DB^3 by varying the sensing radius. In general, the curves of six compared algorithms have a similar trend that the average number of directional sensors decreases with the sensing radius. This occurs because the number of fully covered grids increases with the sensing radius of the directional sensor. Thus a DB^3 can be constructed by a smaller number of directional sensors if each directional sensor has a larger sensing radius. Although the number of partially covered grids $n_{avg}^{partial}$ also increases with the sensing radius, the $n_{avg}^{partial}$ is smaller than n_{avg}^{full} in terms of increasing magnitude, which can be validated in Table 3 and Fig. 12 as well. Fig. 13(a) also shows that the BRA approaches the optimal solution (MDP) and outperforms the CoBRA and D-TriB.

Fig. 13(b) investigates the average number of directional sensors needed for constructing a DB^3 by varying the degree of FoV. In general, the average number of directional sensors decreases with the degree of FoV. This occurs because a directional sensor that has larger degree of FoV can cover more *fully covered grids*. Thus a DB^3 can be constructed by a smaller number of directional sensors if the FoV of each directional sensor has a larger degree. Fig. 13(b) also shows that the proposed BRA approaches the optimal solution (MDP) and outperforms both the CoBRA and the D-TriB in terms of the average number of directional sensors needed for constructing a DB^3.

The success ratio of defense barrier construction will be influenced by the size of grid and by the degree of FoV. Fig. 14 gives a success ratio comparison of a DB^3 construction among BA, BTA, BRA, and MDP by varying both of the size of grid and degree of FoV. As shown in Fig. 14, with the decreasing size of the grid and increasing degree of FoV, the success ratio of a DB^3 construction

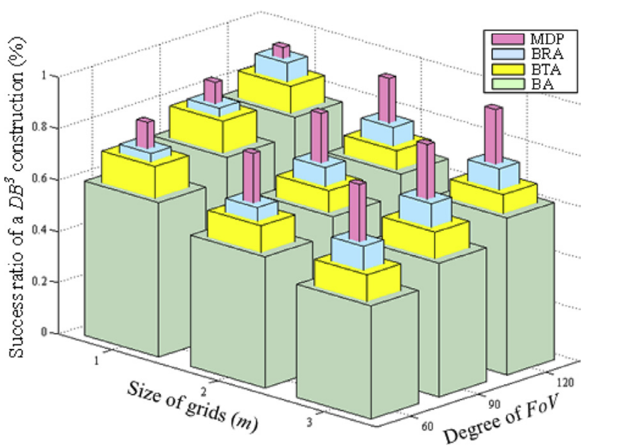

Fig. 14. Performance comparison of MDP, BA, BTA, and BRA in terms of the success ratio of a DB^3 construction by varying both of the size of grid and degree of FoV. The R and $|V|$ are set by $R = 400\text{m} \times 400\text{m}$ and $|V| = 400$, respectively.

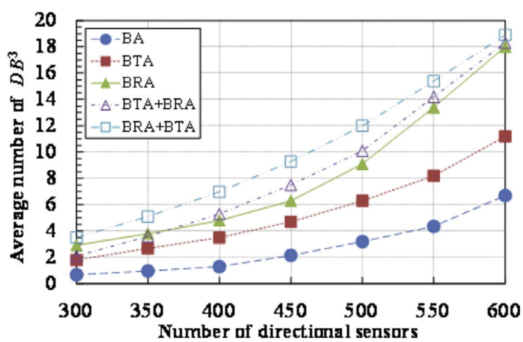

Fig. 15. Performance comparison of BA, BTA, BRA, and their combinations including BTA+BRA and BRA+BTA in terms of average number of DB^3 by varying the number of directional sensors. The R, l, and FoV are set by $R = 400\text{m} \times 400\text{m}$, $l = 1\text{m}$, and $\text{FoV} = \pi/2$, respectively.

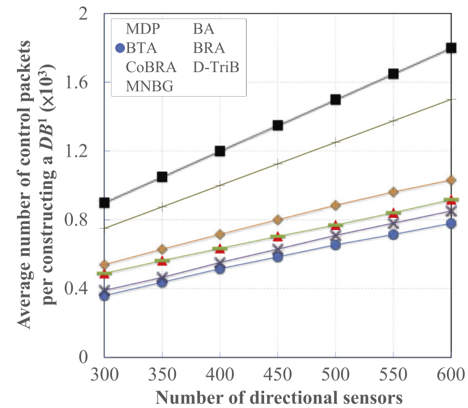

Fig. 16. Performance comparison of BA, BTA, BRA, CoBRA, D-TriB, MDP, and MNBG in terms of the average number of control packets per constructing a DB^1. The R, l, and FoV are set by $R = 400\text{m} \times 400\text{m}$, $l = 1\text{m}$, and $\text{FoV} = \pi/2$, respectively.

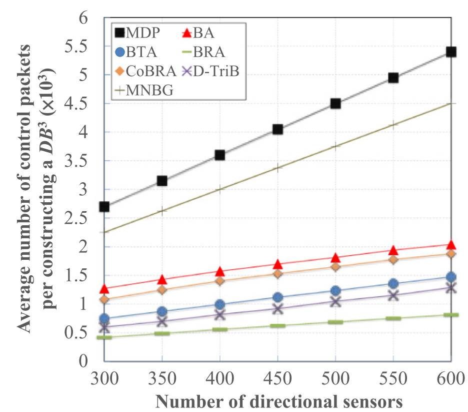

Fig. 17. Performance comparison of BA, BTA, BRA, CoBRA, D-TriB, MDP, and MNBG in terms of the average number of control packets per constructing a DB^3. The R, l, and FoV are set by $R = 400\text{m} \times 400\text{m}$, $l = 1\text{m}$, and $\text{FoV} = \pi/2$, respectively.

increases. This occurs because the small size of the grid and the large degree of FoV will raise the number of grids that can be fully covered by each directional sensor. These extra fully covered grids can be further considered by current decision maker DM^{curr} such that the construction of DB^3 has a larger probability to occur. Fig. 14 also shows that the BRA outperforms the BA and BRA. The major reason is that the BRA can invite more *weak grids* to join the construction of DB^3 than BA and BRA even if the size of grid is large and the degree of FoV is reduced. In addition, the BRA is very close to the optimal solution (MDP) especially when the size of the grid is small and the degree of FoV is large.

It is interesting that the backtracking and branch policies can be integrated to obtain a better performance when constructing a DB^k. Fig. 15 investigates the performance improvement by integrating the BA, BTA, and BRA with different orders. The individual BA, BTA, and BRA are compared with the combinational mechanisms in terms of the number of constructed DB^3. The BTA+BRA mechanism firstly applies the BTA approach to constructing a DB^3 and then further applies the branch approach when DM^{curr} fails to find the next qualified grid. Unlike BTA+BRA mechanism, the BRA+BTA mechanism adopts the branch policy to utilize the weak grids first. Once the DM^{curr} encounters the dead-end problem, the backtracking policy is further applied. In Fig. 15, these two combination mechanisms outperform the other three compared mechanisms in terms of the number of constructed DB^3. The BRA+BTA mechanism has a better performance than BTA+BRA mechanism. This occurs because the branch policy applied first in the BRA+BTA mechanism fully utilizes the weak grids and thus gives more opportunities to construct a successful DB^3.

Fig. 16 investigates the average number of control packets by constructing a DB^1 and varying the number of directional sensors. As shown in Fig. 16, the proposed BTA outperforms the MDP, BA, BRA, CoBRA, D-TriB, and MNBG. The main reason for this is that the proposed BTA adopts a grid partitioning scheme and only requires DMs, instead of all sensor nodes, to participate in the defense barrier construction process. Therefore, the control packet overhead of the proposed BTA are significantly fewer than those of MDP, BA, BRA, CoBRA, D-TriB, and MNBG. In addition, D-TriB and MNBG adopt centralized algorithms which require previous collection of information from the whole network. As a result, D-TriB and MNBG generate a considerable number of control packets.

Fig. 17 further investigates the average number of control packets by constructing a DB^3 and varying the number of directional sensors. As shown in Fig. 17, the results are similar to those of Fig. 16. The proposed BRA outperforms the MDP, BA, BTA, CoBRA, D-TriB, and MNBG. It is notable that the proposed BRA generates fewer number of control overheads than the proposed BTA. This occurs because BRA applies a branch policy which further exploits more barriers than BTA.

7. Conclusion

Barrier coverage is one of the most important issues in intruder detection applications. Directional sensors can support more accurate information regarding an intruder but also raise the problem of large data volume for information exchange and processing. To cope with the problem, constructing a disjoint k-coverage barrier (DB^k) using as few directional sensors as possible is the main goal of barrier coverage problem in DWSNs. This paper presents a k-BCC mechanism with three barrier-construction policies, called BA, BTA, and BRA. Firstly, a decentralized BA mechanism is proposed to deal with the k-barrier coverage problem. In addition to BA, the BTA and BRA algorithms that adopt backtracking and branch policies are proposed to further construct more disjoint k-coverage barrier (DB^k) than BA, for a predefined constant k. Analyses of performance drop caused by *grid partition* and message complexity were also made. The experimental study shows that the proposed BRA outperforms BA and BTA, and likely approaches the optimal solution (MDP) in terms of the number of constructed DB^k when $k \geq 2$. Furthermore, the proposed BRA achieves better performance in terms of the number of control packets and constructed defense barriers, as compared with the existing works [17,19].

Acknowledgment

This work was supported by the Ministry of Science and Technology of Taiwan under Grant MOST 103-2221-E-032-020-MY3 and Grant MOST 106-2221-E-032-015-MY3.

References

[1] R. Holman, J. Stanley, T. Ozkan-Haller, Applying video sensor networks to nearshore environment monitoring, IEEE Trans. Pervasive Comput. 2 (October-December (4)) (2003) 14–21.
[2] W. Feng, B. Code, E. Kaiser, M. Shea, W. Feng, Panoptes: scalable low-power video sensor networking technologies, in: Proc. ACM MM, 2003.
[3] P. Kulkarni, D. Ganesan, P. Shenoy, Q. Lu, SensEye: a multitier camera sensor network, in: Proc. ACM MM, 2005.
[4] Department of Homeland Security [Online]. Available: http://www.dhs.gov/securing-and-managing-our-borders.
[5] R.C. Archibold, 28-mile virtual fence is rising along the border, 2007. New York Times [Online]. Available http://www.nytimes.com/2007/06/26/us/26fence.html?_r=0.
[6] S. Kumar, T.H. Lai, A. Arora, Barrier coverage with wireless sensors, in: Proc. ACM MobiCom, 2005.
[7] S. Kumar, T.H. Lai, M.E. Posner, P. Sinha, Maximizing the lifetime of a barrier of wireless sensors, IEEE Trans. Mobile Comput. 9 (August (8)) (2010) 1161–1172.
[8] A. Chen, S. Kumar, T.H. Lai, Local barrier coverage in wireless sensor networks, IEEE Trans. Mobile Comput. 9 (April (4)) (2010) 491–504.
[9] C.F. Huang, Y.C. Tseng, The coverage problem in a wireless sensor network, in: Proc. ACM WSNA, 2003.
[10] G. Yang, D. Qiao, Multi-round sensor deployment for guaranteed barrier coverage, in: Proc. IEEE INFOCOM, 2010.
[11] B. Liu, O. Dousse, J. Wang, A. Saipulla, Strong barrier coverage of wireless sensor networks, in: Proc. ACM MobiHoc, 2008.
[12] A. Chen, T.H. Lai, D. Xuan, Measuring and guaranteeing quality of barrier coverage for general belts with wireless sensors, ACM Trans. Sens. Netw. 6 (December (1)) (2009).
[13] S. He, X. Gong, J. Zhang, J. Chen, Y. Sun, Barrier coverage in wireless sensor networks: from lined-based to curve-based deployment, in: *Proc. IEEE INFOCOM*, Turin, Italy, April, 2013.
[14] S. He, X. Gong, J. Zhang, J. Chen, Y. Sun, Curve-based deployment for barrier coverage in wireless sensor networks, IEEE Trans. Wireless Commun. 13 (February (2)) (2014) 724–735.
[15] H. Ma, Y. Liu, Some problems of directional sensor networks, J. Sensor Networks 2 (April (1/2)) (2007) 44–52.
[16] L. Zhang, J. Tang, W. Zhang, Strong barrier coverage with directional sensors, in: Proc. IEEE GlobeCom, 2009.
[17] K.P. Shih, C.M. Chou, C.I. Liu, C.C. Li, On Barrier coverage in wireless camera sensor networks, in: Proc. IEEE AINA, 2010.
[18] D. Tao, S. Tang, H. Zhang, X. Mao, H. Ma, Strong barrier coverage in directional sensor networks, Comput. Commun. 35 (May (8)) (2012) 895–905.
[19] C.F. Cheng, K.T. Tsai, Distributed barrier coverage in wireless visual sensor networks with β-QoM, IEEE Sensors J. 12 (June (6)) (2012) 1726–1735.
[20] Z. Wang, J. Liao, Q. Cao, H. Qi, Z. Wang, Barrier coverage in hybrid directional sensor networks, in: Proc. IEEE MASS, 2013.
[21] Z. Wang, J. Liao, Q. Cao, H. Qi, Z. Wang, Achieving k-barrier coverage in hybrid directional sensor networks, IEEE Trans. Mobile Comput. 13 (July (7)) (2014) 1443–1455.
[22] D. Tao, T.Y. Wu, A survey on barrier coverage problem in directional sensor networks, IEEE Sens. J. 15 (February (2)) (2015) 876–885.
[23] A. Schrijver, Combinatorial Optimization: Polyhedra and Efficiency, Springer, 2003 ISBN 978-3-540-44389-6.
[24] W.H.R. Chan, P.F. Zhang, I. Nevat, S.G. Nagarajan, A.C. Valera, H.X. Tan, N. Gautam, Adaptive duty cycling in sensor networks with energy harvesting using continuous-time Markov chain and fluid models, IEEE J. Sel. Areas Commun. 33 (December (12)) (2015) 2687–2700.

Chih-Yung Chang (M'05) received the Ph.D. degree in computer science and information engineering from the National Central University, Zhongli, Taiwan, in 1995.

He is currently a Full Professor with the Department of Computer Science and Information Engineering, Tamkang University, New Taipei City, Taiwan. His current research interests include internet of things, wireless sensor networks, ad hoc wireless networks, and Long Term Evolution (LTE) broadband technologies. He has served as an Associate Guest Editor for several SCI-indexed journals, including the *International Journal of Ad Hoc and Ubiquitous Computing* from 2011 to 2016, the *International Journal of Distributed Sensor Networks* from 2012 to 2014, *IET Communications* in 2011, *Telecommunication Systems* in 2010, the *Journal of Information Science and Engineering* in 2008, and the *Journal of Internet Technology* from 2004 to 2008.

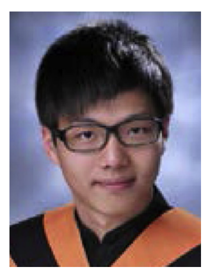

Chih-Yao Hsiao received the B.S. degree and M.S. degree in Computer Science and Information Engineering from I-Shou University in 2009 and Tamkang University in 2011, respectively, Taiwan. He is currently working toward the Ph.D. degree in Computer Science and Information Engineering at Tamkang University. He received several scholarship grants in Taiwan and has participated in many projects related to Wireless Sensor Networks, Vehicular Ad hoc networks, Internet of Things, and Software Defined Networks. His research interests include Internet of Things, Wireless Sensor Networks, Ad Hoc Wireless Networks, and Vehicular Ad Hoc Networks.

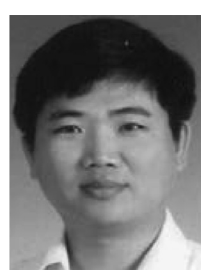

Chao-Tsun Chang (M'12) received the Ph.D. degree in computer science and information engineering from National Central University, Taoyuan, Taiwan, in 2006. He is currently an Associate Professor with the Department of Information Management, Hsiuping University of Science and Technology, Taichung, Taiwan. In the past ten years, he has directed 12 research projects, including five National Science Council projects and seven information system developments. His current research interests include ad hoc wireless networks, wireless sensor networks, internet of things, and mobile computing. Dr. Chang is a member of the IEEE Computer and Communication Societies.